

You never have enough J/ψ events

—The case for a J/ψ factory—

Stephen Lars Olsen

Institute for Basic Science,
Daejeon 34126, Republic of Korea

University of Science and Technology of China,
Hefei 230026, People's Republic of China

June 27, 2025

Abstract

In a talk at an IHEP-Beijing symposium celebrating the 50th anniversary of the discovery of the J/ψ , I reminisced about some of the interesting phenomena that were observed in J/ψ decays in the BES, BESII, and BESIII detectors during the 35 year long BES experimental program. The three order of magnitude increase in the J/ψ event samples and the improved detector capabilities that occurred during this time led to a persistent series of interesting discoveries and new insights. As more J/ψ events were collected, the scientific interest in them increased and the breadth of physics topics that are addressed by them expanded. In addition, I speculated on what might happen if, in the next few decades, the magnitude of J/ψ data samples and the detector capabilities continued to increase at similar paces. In particular, I emphasize the possibilities of searches for \mathcal{CP} violation in strange hyperon decays and testing the \mathcal{CPT} theorem with strangeness-tagged neutral kaon decays.

1 Introduction

“Why do we need more J/ψ events?” and “...don't we already have enough?” are questions that have been frequently asked at collaboration meetings throughout the history of the BES, BESII and, now, BESIII experiments, usually by charm physics aficionados while they are clamoring for more data at the $D\bar{D}$ or $D_s\bar{D}_s$ thresholds, or, more recently, by XYZ -meson enthusiasts with ambitions to find yet another multiquark state. In the past, the answer has been primarily been that the J/ψ is a prolific source of light hadrons that are produced with low backgrounds and well defined quantum numbers that have supported numerous, and often unique, studies of the spectroscopy of light-quark hadrons and the dynamics of their production and decays. Maybe not the most glamorous physics, but still very interesting and useful.

In the mid-1990s, during the early running of BES and with 8 million J/ψ events, we focused on gluon-rich hadronic systems produced radiative J/ψ decays and mapped out the $J^P=0^+$ and 2^+ $\pi^+\pi^-$, $\pi^0\pi^0$ and K^+K^- resonances in the 1.5-2.0 GeV mass

region [1] as well as the pretty intricate $\eta\pi^+\pi^-$ and $K\bar{K}\pi$ systems in the 1.1-2.0 GeV mass range, that covers what are now called the $\eta(1405)/\eta(1475)$ resonances [2]. Some of these three-decade-old papers continue to be of interest and still get occasionally cited [3, 4].

In the BESII era, between 1998 and 2006, 58 million J/ψ events were collected and, with these, we reported what was the strongest evidence at the time for the long-sought for 0^+ σ resonance in $J/\psi \rightarrow \omega\pi^+\pi^-$ decays [5] and its strange counterpart, the κ in $J/\psi \rightarrow \bar{K}^{*0}K^+\pi^-$ decays [6].¹ In addition, we found the curious near-threshold $p\bar{p}$ mass enhancement in $J/\psi \rightarrow \gamma p\bar{p}$ decays shown in Fig. 1a, that, when fitted with a threshold-modified Breit-Wigner function, had a peak mass that was 18 MeV *below* the $2m_p$ threshold with a width that was less than 30 MeV [8], and looked very much like a $p\bar{p}$ bound state. This was followed by the discovery of the $X(1835)$, an $\pi^+\pi^-\eta'$ state with a peak mass in the same region [9] (see Fig. 1b) that was also produced in radiative J/ψ decays. This was interpreted by some authors as a multigluon decay mode of the subthreshold $p\bar{p}$ state [10].

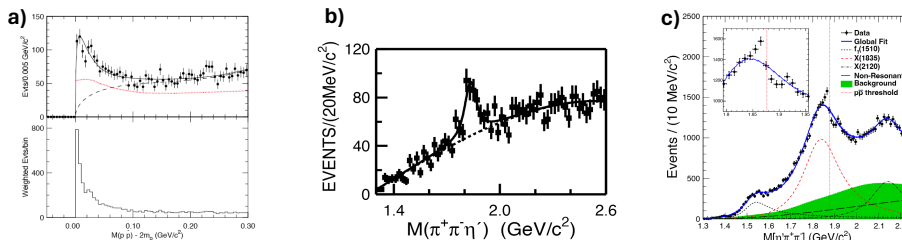


Figure 1: **a)** The upper panel shows the $M(p\bar{p}) - 2m_p$ distribution for $J/\psi \rightarrow \gamma p\bar{p}$ in the 58 M J/ψ event sample [8]. The fitted curve is described in the text. The lower panel shows the same distribution weighted by the inverse of phase space. **b)** The $\pi^+\pi^-\eta'$ invariant mass distribution for $J/\psi \rightarrow \gamma\pi^+\pi^-\eta'$ events in the 58 M J/ψ event sample [9]. **c)** The same distribution for 1.09 B J/ψ events [11]. The blue curve shows results of a fit to the $X(1835)$ peak with a simple Breit-Wigner lineshape.

The BESIII era started operation in 2008, and, with the big boost in statistics provided by 1.09 B events that were collected during our first run at the J/ψ peak, we observed strong interference effects on the high-mass side of $X(1835)$ mass peak that occurred exactly at the $M(\pi^+\pi^-\eta') = 2m_p$ $p\bar{p}$ threshold as shown in Fig. 1c, where the fitted curve assumes a simple Breit-Wigner lineshape and the $p\bar{p}$ threshold is indicated by a dashed vertical line. As more J/ψ events were accumulated, more intriguing details became apparent [11]. At present, this pattern is best described as the interference of a broad resonance peaked near 1835 MeV and a narrow ($\Gamma \sim 10$ MeV) sub-threshold resonance with a peak mass ~ 5 MeV *below* $2m_p$ and with a strong $p\bar{p}$ coupling.

More recently, with 10 B J/ψ events, BESIII found a strong signal for an $\eta\eta'$ resonance with exotic $J^{PC} = 1^{-+}$ quantum numbers in $J/\psi \rightarrow \gamma\eta\eta'$ decays (with 19σ significance!) as shown in Fig. 2a. This state, called the $\eta_1(1855)$, is a prime candidate for an isoscalar $q\bar{q}$ -gluon QCD hybrid state [12].² In addition, with $J/\psi \rightarrow \gamma K^0\bar{K}^0\eta'$ decay events in the same 10 B J/ψ event sample, BESIII found the $X(2370)$, a $K^0\bar{K}^0\eta'$ resonance with $J^{PC} = 0^{-+}$ (see Fig. 2b), with a mass, width and decay properties that closely match theoretical predictions for the lightest pseudoscalar glueball [14].

In addition, with billions of J/ψ events and decays like $J/\psi \rightarrow \phi f_0(980)$ ($\mathcal{B} = 0.03\%$),

¹Renamed as the $f_0(500)$ and $K_0^*(700)$ by the PDG [7].

²Could it be the isoscalar partner of the (also exotic) 1^{-+} $\pi_1(1600)$ candidate hybrid meson [13]?

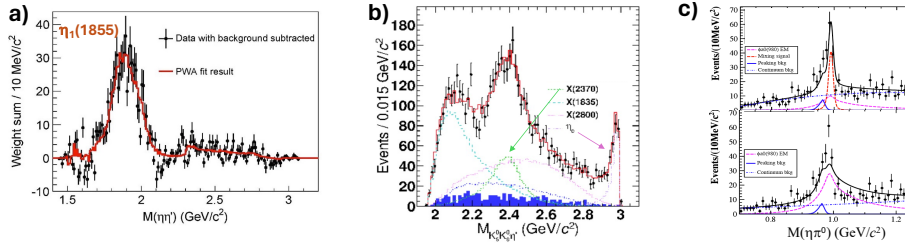


Figure 2: **a)** The 1^{-+} $\eta\eta'$ partial wave for $J/\psi \rightarrow \gamma\eta\eta'$ events [12]. **b)** The $K_S K_S \pi^+ \pi^-$ invariant mass distribution for $J/\psi \rightarrow \gamma K_S K_S \pi^+ \pi^-$ events [14]. **c)** The $\eta\pi^0$ mass spectrum for $J/\psi \rightarrow \phi\eta\pi^0$ events. The top panel shows the results of a fit with $J/\psi \rightarrow \phi f_0(980)$, $f_0 \rightarrow a_0(980) \rightarrow \eta\pi^0$ included and shown as a dashed red curve; the bottom panel shows a fit with mixing excluded. [15].

$\gamma\eta$ ($\mathcal{B}=0.1\%$), & $\gamma\eta'$, ($\mathcal{B}=0.5\%$), BESIII has functioned as a multiple light meson factory with multimillion-event low-background samples of tagged η , η' & $f_0(980)$ decays that have been used to make precision measurements and support studies of a variety of rare processes (see, *e.g.*, [16]).

For example, the $J/\psi \rightarrow \phi f_0(980)$ events provided a large sample of tagged $f_0(980)$ mesons that were used to measure the $f_0 \rightarrow a_0 \rightarrow \eta\pi^0$ mixing process with a significance of 7.4σ as shown in Fig. 2c, [15]. In the same analysis $\psi' \rightarrow \gamma\chi_{c1} \rightarrow \gamma\pi^0 a_0(980)$ decays were used to tag a_0 mesons that were used to measure the $a_0 \rightarrow f_0 \rightarrow \pi^+ \pi^-$ reverse process with 5.5σ significance. These measurement were the first to establish the existence of a_0 - f_0 mixing, which had been predicted some 40 years earlier [17] but had never been seen. In addition, the strengths of the measured $f_0 \rightarrow a_0$ and $a_0 \rightarrow f_0$ couplings strongly supported the four-quark structure of the $f_0(890)$ - $a_0(980)$ nonet of scalar mesons [18], something that has been a subject of numerous discussions in the light hadron community ever since the possibility was first suggested by Bob Jaffe in 1976 [19].

Six years ago, I reviewed some of the above results in a talk that I gave at the IHEP symposium celebrating the 30th anniversary of the start of the BES experimental program, and concluded my remarks with the comment:

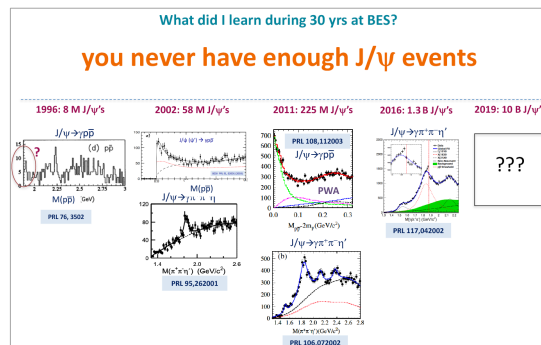


Figure 3: My final slide at the BES 30th anniversary symposium (September 2019).

This comment seemed to strike a resonant chord in the psyche of my BES colleagues because, in spite of the numerous (what I thought were) sage observations that I made

during my many years of participation in BES, this is the only one that seems to be remembered and repeated, and, I suppose, is the reason I was given the honor to speak at this auspicious meeting.

During the BES experimental program, we enjoyed a three order of magnitude increase in the number of J/ψ events we had to work with, and with each major increase we were rewarded with new insights and discoveries. There was never any sign of saturation; as more J/ψ became available, we always found more things to do with them. Given this history, it is interesting to speculate about what might happen if at some post-BESIII, but near-future facility, the next generation of researchers also got to enjoy similar multiple order-of-magnitude boosts in J/ψ event samples and an even more capable detector. An obvious extrapolation from the past is that more light-hadron states would be found, the spectroscopies of QCD glueballs and hybrid mesons would be established and to a large extent mapped out, decays of the η , η' and $f_0(980)/a_0(980)$ mesons would be studied with even higher precision and even rarer process would be found, and, in an era where Lattice QCD and AI will play an increasingly important role in our science, the large number of J/ψ events would enable numerous precision measurements of various quantities that could help calibrate and validate these computations. I won't discuss these today and, instead, point toward two qualitatively different research opportunities that are close to my heart and that multi-trillion J/ψ event samples in a more specialized detector would support: searches for \mathcal{CP} violation in strange hyperon decays and tests of the \mathcal{CPT} theorem with strangeness-tagged K^0 and \bar{K}^0 decays.

2 Why \mathcal{CP} violations in hyperon decays?

The only source of \mathcal{CP} violation in the SM is the Kobayashi-Maskawa phase in the CKM quark-flavor mixing matrix, and this has provided precise quantitative explanations for virtually all experimentally observed \mathcal{CP} -violating phenomena, including \mathcal{CP} -symmetry violations in the decays of strange and bottom-flavored hadrons. However the KM \mathcal{CP} -violating mechanism cannot explain how the current all-matter universe evolved from what had to have been a matter-antimatter symmetric condition that existed shortly after the Big Bang. KM-model-based calculations fail to account for the baryon asymmetry of the current universe—commonly referred to as the BAU—by some ten orders of magnitude [20]. Thus, there must have been other, non-SM source (or sources) of \mathcal{CP} violation in Nature.

Searches for anomalous \mathcal{CP} violations in the b - and c -quark sectors are the major motivations for the LHCb experiment [21] at CERN Large Hadron Collider and the Belle II experiment [22] at KEK. Although many \mathcal{CP} -violations have been established in the b -quark sector, so far at least, these can all be explained by the KM mechanism [23], including the recently seen \mathcal{CP} violation in $\Lambda_B \rightarrow p K^- \pi^+ \pi^-$ decay [24] (see ref. [25]). For a long time, theorists assured experimentalists that \mathcal{CP} violating asymmetries in the c -quark sector larger than $\sim 0.01\%$ could not be explained by the KM-mechanism and would be clear evidence for new, beyond-the-SM physics [26]. This confidence lasted until a few days after the LHCb group announced evidence for a huge, nonzero \mathcal{CP} -violating asymmetry in $D \rightarrow K^+ K^-$ and $\pi^+ \pi^-$ decay in 2011 [27], which was followed by a 5σ discovery of a no-longer huge—but still large— \mathcal{CP} violation in 2019 [28]:

$$\frac{\mathcal{B}(D \rightarrow K^+ K^-) - \mathcal{B}(\bar{D} \rightarrow K^+ K^-)}{\mathcal{B}(D \rightarrow K^+ K^-) + \mathcal{B}(\bar{D} \rightarrow K^+ K^-)} - \frac{\mathcal{B}(D \rightarrow \pi^+ \pi^-) - \mathcal{B}(\bar{D} \rightarrow \pi^+ \pi^-)}{\mathcal{B}(D \rightarrow \pi^+ \pi^-) + \mathcal{B}(\bar{D} \rightarrow \pi^+ \pi^-)} = -(0.15 \pm 0.03)\%.$$

Regrettably, instead of being endorsed as new physics discoveries, this \mathcal{CP} violation was attributed to SM processes enhanced by $SU(3)$ -violating K^+K^- and $\pi^+\pi^-$ final-state interactions (see refs. [29] and [30]), *i.e.*, SM light-hadron physics in the 1.8–1.9 GeV mass region (that was very familiar to old-timers in the BES collaboration).

Stringent limits on flavor conserving non-SM \mathcal{CP} violations in the (u, d) light quark sector have been established by very sensitive searches for electric dipole moments of the neutron [31] and the electron [32, 33]. And, despite a barrage of public statements to the contrary, there is no possible value of the Dirac phase in the PMNS neutrino-mixing matrix that could be measured by impending long-baseline neutrino experiments [34, 35] that could resolve the BAU conundrum [36].

That leaves us with \mathcal{CP} violations in the s -quark sector, where the only direct \mathcal{CP} -violation that has been seen so far is the one characterized by the parameter ε' that was measured as a small, nonzero effect in $K_L \rightarrow \pi\pi$ decay by the NA48 experiment at CERN [37] and the KTeV experiment at Fermilab [38]. This parameter quantifies the \mathcal{CP} -violating phase difference between interfering isospin = 2 and isospin = 0, parity-violating S -wave amplitudes in $K^0(\bar{K}^0) \rightarrow \pi\pi$ decays, and is suppressed in magnitude by a nominal factor of 1/22.5 by the weak-interaction's $\Delta I=1/2$ rule. The \mathcal{CP} -phase difference³ between the I=2 and I=0 S -wave $K \rightarrow \pi\pi$ amplitudes that is deduced⁴ from the measured value of ε' is $\xi_{K \rightarrow \pi\pi}^S \approx 0.005^\circ$, and is within errors of the SM prediction [39] $\xi_{K \rightarrow \pi\pi}^S(SM) \approx 0.004^\circ$.

But this only constrains new physics sources of \mathcal{CP} violations in in parity-violating S -wave amplitudes. Hyperon decays involve interfering S - and P -wave amplitudes. The measured \mathcal{CP} -phase in $K \rightarrow \pi\pi$ decay and its agreement with SM expectations has been translated [40, 41] into stringent limits on contributions from BSM new physics sources to the S -wave amplitudes in hyperon decays that imply that any observed \mathcal{CP} violation at the current levels of experimental sensitivity would correspond to new physics contributions to the parity-conserving P -wave amplitudes.

2.1 $e^+e^- \rightarrow J/\psi \rightarrow \Xi \bar{\Xi}$, near-perfect fits for hyperon \mathcal{CP} studies

Figure 4a shows what an $e^+e^- \rightarrow J/\psi \rightarrow \Xi^- \bar{\Xi}^+$, where $\Xi^- \rightarrow \Lambda\pi^-$, $\Lambda \rightarrow p\pi^-$, and $\bar{\Xi}^+ \rightarrow \bar{\Lambda}\pi^+$, $\bar{\Lambda} \rightarrow \bar{p}\pi^+$ event looks like in the BESIII detector; Fig. 4b shows a roadmap of the underlying decay chains. These events, along with their $\Xi^0 \bar{\Xi}^0$ isospin counterparts, are nearly perfect reactions for studying hyperon \mathcal{CP} violations for the following reasons:

- i)* the Ξ and $\bar{\Xi}$ are in a mixture of $J^P=1^-$ quantum states with $J_z=\pm 1$ but not $J_z=0$;
- ii)* \mathcal{P} conservation in their production makes the Ξ & $\bar{\Xi}$ polarizations exactly equal;
- iii)* \mathcal{P} violation in Λ & $\bar{\Lambda}$ decay provide event-by-event Λ & $\bar{\Lambda}$ spin measurements;
- iv)* quantum correlations & Λ spin measurements make the effective polarizations=1;
- v)* the Ξ and $\bar{\Xi}$ are back-to-back in a symmetric detector with equal momenta;
- vi)* Ξ and $\bar{\Xi}$ decay products have identical fiducial volumes and selection requirements;
- vii)* most of the Ξ & $\bar{\Xi}$ decays occur in a vacuum.

³Unlike zillions of other phases in physics, a \mathcal{CP} phase has opposite sign for particles and antiparticles.

⁴This is $\xi_{K \rightarrow \pi\pi}^S \approx 22.5 \times \sqrt{2} \operatorname{Re}(\varepsilon'/\varepsilon) \times \varepsilon$, where $|\operatorname{Im} A_{\pi\pi}^{I=2}| = \sqrt{2} |\operatorname{Re}(\varepsilon'/\varepsilon)|$, of which $\operatorname{Re}(\varepsilon'/\varepsilon) = 1.7 \times 10^{-3}$ is what is measured, $\varepsilon = 2.23 \times 10^{-3}$ is the neutral kaon mass-matrix \mathcal{CP} -violating parameter, and the 22.5 factor accounts for the larger $\Delta I=1/2$ interfering $A_{\pi\pi}^{I=0}$ amplitude.

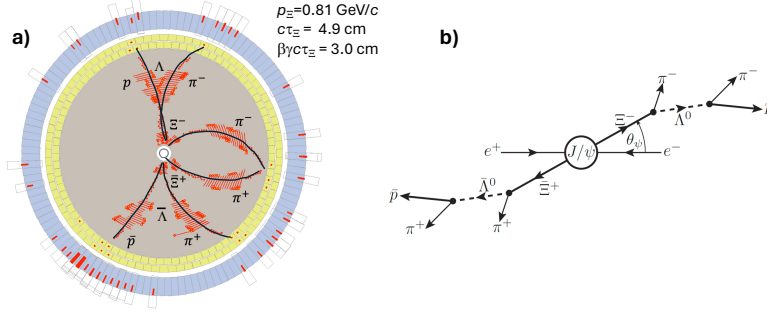


Figure 4: a) An $e^+e^- \rightarrow J/\psi \rightarrow \Xi^- \bar{\Xi}^+$ event in the BESIII detector. b) A road map for these events.

The overall process involves five different reactions that are most simply described by considering five different reference frames. The first is the J/ψ rest frame where, since the spin=1 J/ψ mesons are produced in e^+e^- annihilation via a single virtual photon, they are spin-aligned along the direction of the e^+e^- beamline (taken as the z axis). This means that equal numbers of them are produced in the $|J; J_z\rangle = |1; +1\rangle$ and $|1; -1\rangle$ angular momentum states, but none with $|J; J_z\rangle = |1; 0\rangle$. The $J/\psi \rightarrow \Xi \bar{\Xi}$ decay matrix element is the sum of two helicity amplitudes. The interference between these two amplitudes and the absence of any initial-state $J_z=0$ component produces a θ_{ψ} -dependent production cross section for Ξ & $\bar{\Xi}$ hyperons that are spin-polarized with polarizations $\vec{\mathcal{P}}_{\Xi}$ that are perpendicular to the production plane: [42]:

$$\frac{1}{N} \frac{dN}{d \cos \theta_{\psi}} = \frac{3}{4\pi} \frac{1 + \alpha_{\psi} \cos^2 \theta_{\psi}}{3 + \alpha_{\psi}} \quad (1)$$

$$\vec{\mathcal{P}}_{\Xi} = \frac{\sqrt{1 - \alpha_{\psi}^2} \sin \theta_{\psi} \cos \theta_{\psi} \sin \Delta\Phi}{1 + \alpha_{\psi} \cos^2 \theta_{\psi}}, \quad (2)$$

where α_{ψ} is a parity- and \mathcal{CP} -conserving parameter that characterizes the relative strengths of the two helicity amplitudes, $\Delta\Phi$ is their relative phase, and the polarizations of the hyperons are equal, *i.e.*, $\vec{\mathcal{P}}_{\Xi} = \vec{\mathcal{P}}_{\bar{\Xi}}$.

The next two reference frames to consider are the Ξ and $\bar{\Xi}$ rest frames. In these frames the decay angle θ_{Λ} ($\theta_{\bar{\Lambda}}$) relative to \mathcal{P}_{Ξ} direction, and the polarization vectors of the Λ daughters ($\vec{\mathcal{P}}_{\Lambda}$) and ($\vec{\mathcal{P}}_{\bar{\Lambda}}$), are distributed according to [43]

$$\frac{dN}{d \cos \theta_{\Lambda}} \propto 1 + \alpha_{\Xi} \mathcal{P}_{\Xi} \cos \theta_{\Lambda} \quad (3)$$

$$\mathcal{P}_{\Lambda} = \frac{(\alpha_{\Xi} + \mathcal{P}_{\Xi} \cos \theta_{\Lambda}) \hat{z} + \mathcal{P}_{\Xi} \beta_{\Xi} \hat{x} + \mathcal{P}_{\Xi} \gamma_{\Xi} \hat{y}}{1 + \alpha_{\Xi} \mathcal{P}_{\Xi} \cos \theta_{\Lambda}}, \quad (4)$$

where the unit vectors \hat{x} , \hat{y} , \hat{z} are oriented along the axes indicated in Fig. 5a and α , β , γ are the Lee-Yang decay parameters that are defined below.

The last two reference frames are the Λ and $\bar{\Lambda}$ rest frames. Here the distribution of events in θ_p ($\theta_{\bar{p}}$), the direction of the proton relative to the Λ polarization vector (see Fig. 5b), is

$$\frac{dN}{d \cos \theta_p} \propto 1 + \alpha_{\Lambda} \mathcal{P}_{\Lambda} \cos \theta_p. \quad (5)$$

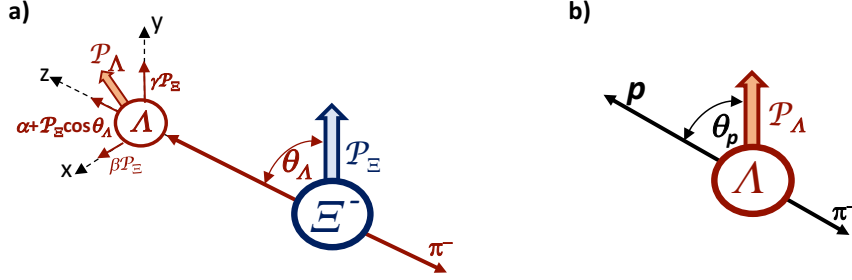


Figure 5: a) The decay angle θ_Λ and Λ polarization vector \mathcal{P}_Λ for polarized $\Xi^- \rightarrow \Lambda\pi^-$ decays. b) The decay angle θ_p for polarized $\Lambda \rightarrow p\pi^-$ decays.

Since the proton and antiproton polarizations are not measured, only the α_Λ and $\alpha_{\bar{\Lambda}}$ parameters can be determined

The (real) Lee-Yang parameters α_Y , β_Y and γ_Y are defined in terms of the (complex) S - and P -wave decay amplitudes S_Y and P_Y as [43]

$$\alpha_Y = \frac{2 \operatorname{Re}(S_Y^* P_Y)}{|S_Y|^2 + |P_Y|^2}, \quad \beta_Y = \frac{2 \operatorname{Im}(S_Y^* P_Y)}{|S_Y|^2 + |P_Y|^2}, \quad \gamma_Y = \frac{|S_Y|^2 - |P_Y|^2}{|S_Y|^2 + |P_Y|^2}, \quad (6)$$

where $Y = \Xi$ or Λ and $\alpha_Y^2 + \beta_Y^2 + \gamma_Y^2 = 1$. The S_Y and P_Y decay amplitudes can have two distinct types of phases. One type corresponds to the S - and P -wave $\Lambda\pi$ and $p\pi$ final-state strong interaction phase shifts, $\delta_{y\pi}^S$ & $\delta_{y\pi}^P$, where $Y \rightarrow y\pi$ ($y = \Lambda$ or p), and have the *same sign* for particles and antiparticles. If \mathcal{CP} is violated, they will have additional so-called *weak*-, or \mathcal{CP} -phases ξ_Y^P and ξ_Y^S that have *opposite signs* for particles and antiparticles. Thus, α_Y (hyperon) and $\alpha_{\bar{Y}}$ (anti-hyperon) have the form[44]

$$\begin{aligned} \alpha_Y &= \frac{2|S_Y||P_Y| \cos((\delta_{y\pi}^P - \delta_{y\pi}^S) + (\xi_Y^P - \xi_Y^S))}{|S_Y|^2 + |P_Y|^2} \\ \alpha_{\bar{Y}} &= -\frac{2|S_Y||P_Y| \cos((\delta_{y\pi}^P - \delta_{y\pi}^S) - (\xi_Y^P - \xi_Y^S))}{|S_Y|^2 + |P_Y|^2}, \end{aligned} \quad (7)$$

where the overall minus sign in the expression for $\alpha_{\bar{Y}}$ comes from the operation of the parity operator (*i.e.* the \mathcal{P} in \mathcal{CP}) on the P -wave amplitude. Thus, assuming $\xi_Y^P - \xi_Y^S$ is small,

$$\mathcal{A}_{\mathcal{CP}}^Y \equiv \frac{\alpha_Y + \alpha_{\bar{Y}}}{\alpha_Y - \alpha_{\bar{Y}}} \approx -\sin(\delta_{y\pi}^P - \delta_{y\pi}^S)(\xi_Y^P - \xi_Y^S), \quad (8)$$

and, if \mathcal{CP} is not conserved, $\xi_Y^P \neq \xi_Y^S$, and any significant difference between $\mathcal{A}_{\mathcal{CP}}^Y$ and zero would unambiguously evidence for a \mathcal{CP} violation.

However, it is evident from eqn. 8 that even if $\xi_Y^P - \xi_Y^S$ is nonzero, $\mathcal{A}_{\mathcal{CP}}^Y$ would be zero if $\delta_{y\pi}^P - \delta_{y\pi}^S = 0$. Although it is unlikely that these strong-interaction phase-shift differences are exactly zero, they are known to be small—theoretical estimates are [45] $\delta_{p\pi}^P - \delta_{p\pi}^S = -7.3^\circ \pm 1.2^\circ$ and [46] $\delta_{\Lambda\pi}^P - \delta_{\Lambda\pi}^S = 8.8^\circ \pm 2.2^\circ$ —and these will suppress the values of $\mathcal{A}_{\mathcal{CP}}^Y$ by an order of magnitude. This is not the case for measurements of the parameter β_Ξ that can be determined from the measurement of \mathcal{P}_Λ in $\Xi \rightarrow \Lambda\pi$ decays. Here, we apply the above-described calculation to a different asymmetry parameter $\mathcal{B}_{\mathcal{CP}}^\Xi$, where

$$\mathcal{B}_{\mathcal{CP}}^\Xi \equiv \frac{\beta_\Xi + \alpha_\Xi}{\alpha_\Xi - \alpha_{\bar{\Xi}}} = \tan(\xi_\Xi^P - \xi_\Xi^S) \approx \xi_\Xi^P - \xi_\Xi^S. \quad (9)$$

In this case the measured asymmetry doesn't suffer any dilution by small strong-interaction phase-shifts. In $\Xi\bar{\Xi}$ events where all the tracks in the decay chain are detected and reconstructed, β_{Ξ} , $\beta_{\bar{\Xi}}$ and \mathcal{B}_{CP}^{Ξ} can be measured. This is only possible with Ξ decays. The Λ and Σ hyperons produced via the $J/\psi \rightarrow \Lambda\bar{\Lambda}$ or $\Sigma\bar{\Sigma}$ reactions decay to nucleons and antinucleons, and precision polarization measurements of nucleons are difficult and impossible for antinucleons.

Since the β_{Ξ} and γ_{Ξ} parameters are not independent, BESIII reports measurements of ϕ_{Ξ} (and $\phi_{\bar{\Xi}}$) that were defined by Lee and Yang to be [43]

$$\beta_{\Xi} = \sqrt{1 - \alpha_{\Xi}^2} \sin \phi_{\Xi} \quad \text{and} \quad \gamma_{\Xi} = \sqrt{1 - \alpha_{\Xi}^2} \cos \phi_{\Xi}. \quad (10)$$

In terms of $\Delta\phi_{CP}^{\Xi} \equiv \frac{1}{2}(\phi_{\Xi} + \phi_{\bar{\Xi}})$ and $\langle\phi_{CP}^{\Xi}\rangle \equiv \frac{1}{2}(\phi_{\Xi} - \phi_{\bar{\Xi}})$:

$$\begin{aligned} \xi_{\Xi}^P - \xi_{\Xi}^S &= \frac{\sqrt{1 - \alpha_{\Xi}^2}}{\alpha_{\Xi}} \Delta\phi_{CP}^{\Xi} = -2.43 \Delta\phi_{CP}^{\Xi} \\ \delta_{\Lambda\pi}^P - \delta_{\Lambda\pi}^S &= \frac{\sqrt{1 - \alpha_{\Xi}^2}}{\alpha_{\Xi}} \langle\phi_{CP}^{\Xi}\rangle = -2.43 \langle\phi_{CP}^{\Xi}\rangle, \end{aligned} \quad (11)$$

where, in the far r.h.s. relation α_{Ξ} was set at -0.38 .

2.2 The BESIII $\Xi^{-}\bar{\Xi}$ and $\Xi^0\bar{\Xi}^0$ event samples

In the BESIII measurement, the Ξ hyperons occur in the reaction chains shown in Fig.4. Here the J/ψ mesons are produced (nearly) at rest in the laboratory by counter-circulating e^+ and e^- beams in the BEPCII collider and the Ξ & $\bar{\Xi}$ are produced back-to-back, in a spin-correlated quantum-entangled state that persists until one of them decays, which usually occurs within a few centimeters of the production point and in a vacuum. In the selected events, both of the Ξ hyperons decay to a pion and a Λ hyperon that, in turn, decays into a charged pion and a proton also within about a few centimeters of the parent Ξ decay points. The events show up in the detector as $p\pi^-$ and $\bar{p}\pi^+$ decay products of nearly back-to-back Λ and $\bar{\Lambda}$ hyperons that are accompanied by two low momentum π^- and π^+ tracks in the case of $\Xi^-\bar{\Xi}^+$ events, and one low momentum π^- and π^+ track and two low-energy $\pi^0 \rightarrow \gamma\gamma$ decays for $\Xi^0\bar{\Xi}^0$ events. The detected events have a very clear topology, with highly constrained kinematics and no particle identification requirements: the highest momentum positive and negative tracks are always the proton and antiproton. The BESIII 10 B J/ψ -event data sample contained 576 k fully reconstructed $\Xi^-\bar{\Xi}^+$ events with less than 0.5% background, and 321 k $\Xi^0\bar{\Xi}^0$ events with less than 2% percent background.

2.3 Analysis and results

The simplicity of the event topology belies a rather intricate analysis. Nine angular measurements are needed to completely specify the kinematics of the event: the production angle, θ_{ψ} , and a pair of angles, θ_Y & φ_Y for each of the four hyperon decay vertices (see Fig. 6). The function that describes these highly correlated angular distributions is characterized by eight parameters: α_{ψ} & $\Delta\Phi$ for the $J/\psi \rightarrow \Xi\bar{\Xi}$ decay vertex, two parameters for each Ξ decay and one parameter for each Λ decay (in which the proton polarization is not measured). The measured quantities are expressed as a

nine-component vector ξ and the angular distribution by an eight-component vector ω :

$$\xi = (\theta_\psi, \theta_\Lambda, \varphi_\Lambda, \theta_{\bar{\Lambda}}, \varphi_{\bar{\Lambda}}, \theta_p, \varphi_p, \theta_{\bar{p}}, \varphi_{\bar{p}}) \quad (12)$$

$$\omega = (\alpha_\psi, \Delta\Phi, \alpha_\Xi, \phi_\Xi, \alpha_{\bar{\Xi}}, \phi_{\bar{\Xi}}, \alpha_\Lambda, \alpha_{\bar{\Lambda}}). \quad (13)$$

Perotti *et al.* [42] provide a modularized expression for the nine dimensional probability distribution that is in a convenient form for symbolic computing:

$$\mathcal{W}(\xi : \omega) = \sum_{\mu\nu=0}^3 C_{\mu\nu} \left(\sum_{\mu'=0}^3 a_{\mu\mu'}^{\Xi} a_{\mu'0}^{\Lambda} \right) \left(\sum_{\nu'=0}^3 a_{\nu\nu'}^{\bar{\Xi}} a_{\nu'0}^{\bar{\Lambda}} \right), \quad (14)$$

where $C_{\mu\nu}$ is a 4×4 matrix that contains the θ_ψ -dependent Ξ & $\bar{\Xi}$ polarizations and spin correlations, and each $a_{\alpha\alpha'}^Y$ represents a 4×4 matrix with elements that contain expressions that involve α_Y & ϕ_Y parameters and Wigner D-functions of the θ_Y, φ_Y angular variables. The second subscript of the $a_{\nu\nu'}^{\Lambda/\bar{\Lambda}}$ terms are zero because the p & \bar{p} polarizations are not measured. The sums in eqn. 14 involve a total of 256 expressions, of which 100 are nonzero.

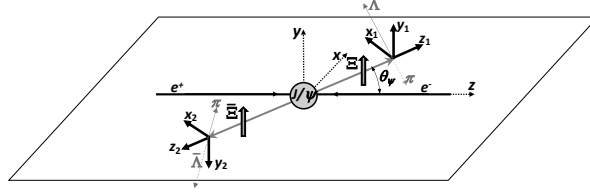


Figure 6: Coordinate systems for $J/\psi \rightarrow \Xi \bar{\Xi}$ and $\Xi \rightarrow \Lambda \pi$ and $\bar{\Xi} \rightarrow \bar{\Lambda} \pi$ decays. The coordinate systems for $\Lambda \rightarrow p \pi^-$ and $\bar{\Lambda} \rightarrow \bar{p} \pi^+$ decays are not shown.

The $C_{\mu\nu}$ spin-density matrix in eqn. 14 has the form

$$C_{\mu\nu}(\theta_\psi, \alpha_\psi, \Delta\Phi) = 2(1 + \alpha_\psi \cos^2 \theta_\psi) \begin{pmatrix} 1 & 0 & \mathcal{P}_y & 0 \\ 0 & C_{xx} & 0 & C_{xz} \\ -\mathcal{P}_y & 0 & C_{yy} & 0 \\ 0 & -C_{xz} & 0 & C_{zz} \end{pmatrix}, \quad (15)$$

where the 0th row is the polarization four-vector⁵ of the Ξ in the (x_1, y_1, z_1) coordinate system in Fig. 6; the 0th column is the same quantity for the $\bar{\Xi}$ in the (x_2, y_2, z_2) system, and the 3×3 submatrix C_{ij} contains the Ξ - $\bar{\Xi}$ spin-correlation coefficients. Parity conservation in the $\Xi \bar{\Xi}$ production process requires that only \mathcal{P}_y and $\bar{\mathcal{P}}_y$ are nonzero and $\mathcal{P}_y = \bar{\mathcal{P}}_y$ if referenced to the (x, y, z) J/ψ rest frame coordinate system.⁶

Figure 7 show the $\cos \theta_\psi$ -dependence of the Ξ polarization and the C_{xx}, C_{yy} and C_{zz} correlations coefficients for $\Xi^- \bar{\Xi}^+$ events. Note that although the average polarization is zero, its rms value is nonzero at $\langle \mathcal{P}_y^\Xi \rangle_{\text{rms}} = 22.3\%$. If the proton and antiproton directions from secondary Λ and $\bar{\Lambda}$ decays are not included in the fit, the 3×3 C_{ij} correlations do not apply, ϕ_Ξ and $\phi_{\bar{\Xi}}$ could not be determined, and the α_Ξ and $\alpha_{\bar{\Xi}}$ measurement sensitivities would be reduced by a factor equal to $\langle \mathcal{P}_y^\Xi \rangle_{\text{rms}}$. With the inclusion of the p & \bar{p} measurements, the C_{ij} correlations come into play, ϕ_Ξ & $\phi_{\bar{\Xi}}$ are

⁵The polarization four vector is defined as $(1, \mathcal{P}_x, \mathcal{P}_y, \mathcal{P}_z)$.

⁶The minus sign in $C_{20} = -\mathcal{P}_y$ reflects the opposite directions of the y_1 & y_2 axes in Fig. 6.

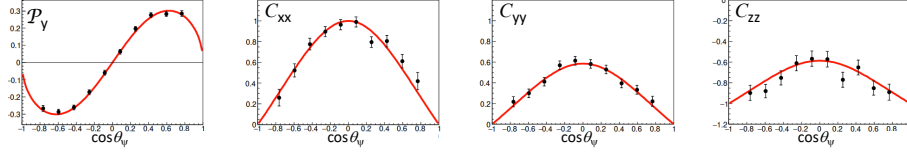


Figure 7: Ξ polarization \mathcal{P}_y and the $\Xi\bar{\Xi}$ spin correlations C_{xx} , C_{yy} and C_{zz} in quantum entangled $J/\psi \rightarrow \Xi^-\bar{\Xi}^+$ events. (From BESIII [47].)

measured, and the effective Ξ polarizations for the α_{Ξ} & $\alpha_{\bar{\Xi}}$ determinations become $\mathcal{P}_y^{\text{eff}}=1$. The corresponding overall sensitivity gain from the Λ polarization measurements is equivalent to a twentyfold increase in the number of events.

Table 1: Results from the BESIII $\Xi^0\bar{\Xi}^0$ analysis and the errors from their $\Xi^-\bar{\Xi}^+$ analysis.

Parameter	$\Xi^0(\Lambda\pi^0)\bar{\Xi}^0(\Lambda\pi^0)$ [48]	$\Xi^-(\Lambda\pi^-\bar{\Xi}^+(\Lambda\pi^+)$ [49]
Number of events	327,305	576,357
α_{ψ}	$0.514 \pm 0.006 \pm 0.015$	$\dots \pm 0.0043 \pm 0.0035$
$\Delta\Phi$ (rad.)	$1.168 \pm 0.019 \pm 0.018$	$\dots \pm 0.0161 \pm 0.0091$
α_{Ξ}	$-0.3750 \pm 0.0034 \pm 0.0016$	$\dots \pm 0.0026 \pm 0.0008$
$\alpha_{\bar{\Xi}}$	$0.3790 \pm 0.0034 \pm 0.0021$	$\dots \pm 0.0026 \pm 0.0007$
ϕ_{Ξ} (rad.)	$0.0051 \pm 0.0096 \pm 0.0018$	$\dots \pm 0.0072 \pm 0.0012$
$\phi_{\bar{\Xi}}$ (rad.)	$-0.0053 \pm 0.0097 \pm 0.0019$	$\dots \pm 0.0072 \pm 0.0016$
α_{Λ}	$0.7551 \pm 0.0052 \pm 0.0023$	$\dots \pm 0.0038 \pm 0.0014$
$\alpha_{\bar{\Lambda}}$	$-0.7448 \pm 0.0052 \pm 0.0017$	$\dots \pm 0.0038 \pm 0.0016$
$\xi_P - \xi_S$ (rad.)	$(0.0 \pm 1.7 \pm 0.2) \times 10^{-2}$	$(\dots \pm 1.2 \pm 0.2) \times 10^{-2}$
$\delta_P - \delta_S$ (rad.)	$(-1.3 \pm 1.7 \pm 0.4) \times 10^{-2}$	$(\dots \pm 1.2 \pm 0.2) \times 10^{-2}$
$A_{\mathcal{CP}}^{\Xi}$	$(-5.4 \pm 6.5 \pm 3.1) \times 10^{-3}$	$(\dots \pm 4.8 \pm 1.4) \times 10^{-3}$
$\Delta\phi_{\mathcal{CP}}^{\Xi}$ (rad.)	$(-0.1 \pm 6.9 \pm 0.9) \times 10^{-3}$	$(\dots \pm 5.1 \pm 1.0) \times 10^{-3}$
$A_{\mathcal{CP}}^{\Lambda}$	$(6.9 \pm 5.8 \pm 1.8) \times 10^{-3}$	$(\dots \pm 4.3 \pm 1.4) \times 10^{-3}$
$\langle\alpha_{\Xi}\rangle$	$-0.3770 \pm 0.0024 \pm 0.0014$	$\dots \pm 0.0018 \pm 0.0005$
$\langle\phi_{\Xi}\rangle$ (rad.)	$0.0052 \pm 0.0069 \pm 0.0016$	$\dots \pm 0.0050 \pm 0.0009$
$\langle\alpha_{\Lambda}\rangle$	$-0.7499 \pm 0.0029 \pm 0.0013$	$\dots \pm 0.0021 \pm 0.0011$

The results of BESIII analyses of the 321 k $\Xi^0\bar{\Xi}^0$ and the errors of 576 k $\Xi^-\bar{\Xi}^+$ event sample are summarized in Table 1. (The $\Xi^-\bar{\Xi}^+$ analysis is complete and the results are known within the BESIII collaboration but, until they are published, only the errors have been released to the public.) Of particular note are the BESIII measurements of ϕ_{Ξ} and $\phi_{\bar{\Xi}}$ that, in degrees, are

Channel	ϕ_{Ξ}	$\phi_{\bar{\Xi}}$	$\xi_P - \xi_S$
$\Xi^0\bar{\Xi}^0$	$0.29^\circ \pm 0.55^\circ \pm 0.10^\circ$	$-0.30^\circ \pm 0.56^\circ \pm 0.11^\circ$	$0.00^\circ \pm 0.97^\circ \pm 0.11^\circ$
$\Xi^-\bar{\Xi}^+$	$\dots^\circ \pm 0.41^\circ \pm 0.07^\circ$	$\dots^\circ \pm 0.41^\circ \pm 0.09^\circ$	$\dots^\circ \pm 0.68^\circ \pm 0.11^\circ$

and, when the Ξ^0 and $\Xi^-\bar{\Xi}^+$ $\xi_P - \xi_S$ values are combined,⁷ we get a sub-1° upper limit:

$$|\xi_P - \xi_S| = 0.00^\circ \pm 0.56^\circ \pm 0.11^\circ < 0.94^\circ \quad (90\% \text{ C.L.}), \quad (16)$$

that is limited by statistical errors. A similar average on the $\delta_P - \delta_S$ strong phase difference results in very nearly the same upper limit

$$|\delta_P - \delta_S| < 1^\circ \quad (90\% \text{ C.L.}), \quad (17)$$

⁷For eqns. 16 and 17, the $\Xi^-\bar{\Xi}^+$ and $\Xi^0\bar{\Xi}^0$ analyses central values were assumed to be that same.

which is much smaller than the $\sim 8.8^\circ$ estimate given in ref. [46] that was mentioned above. According to the definition given above in eqn. 8, this low value of $\delta_P - \delta_S$ means that $|A_{\mathcal{CP}}^\Xi|$ will be $\lesssim 0.02(\xi_P - \xi_S)$ and in all likelihood too small to be a useful probe for \mathcal{CP} violations.

On the other hand, according to eqn. 4 and Fig. 5a, the Λ hyperons produced in $\Xi \rightarrow \Lambda \pi$ decays have a polarization $|\mathcal{P}_\Lambda| \approx |\alpha_\Xi| = 0.38$, that is twice the $\langle \mathcal{P}_y^\Lambda \rangle_{\text{rms}} = 18.7\%$ polarization of lambdas that are produced directly via the $e^+e^- \rightarrow J/\psi \rightarrow \Lambda \bar{\Lambda}$ reaction. As a result, it is interesting to compare measurements of $A_{\mathcal{CP}}^\Lambda$ listed in Table 1 from the 327 k event $\Xi^0 \bar{\Xi}^0$ and 576 k event $\Xi^- \bar{\Xi}^+$ analyses with a BESIII result based on an analysis of 3.23 M $J/\psi \rightarrow \Lambda \bar{\Lambda}$ events [50]:

$$\Xi^0 \bar{\Xi}^0 : A_{\mathcal{CP}}^\Lambda = (6.9 \pm 5.8 \pm 1.8) \times 10^{-3} \quad 327 \text{ k evts} \quad (18)$$

$$\Xi^- \bar{\Xi}^+ : A_{\mathcal{CP}}^\Lambda = (\dots \pm 4.3 \pm 1.4) \times 10^{-3} \quad 576 \text{ k evts} \quad (19)$$

$$\Lambda^0 \bar{\Lambda}^0 : A_{\mathcal{CP}}^\Lambda = (-2.5 \pm 4.6 \pm 1.2) \times 10^{-3} \quad 3.23 \text{ M evts.} \quad (20)$$

Despite having much smaller data samples, the $J/\psi \rightarrow \Xi \bar{\Xi}$ event samples provide independent measurements of $A_{\mathcal{CP}}^\Lambda$ that are similar in precision to those based on $J/\psi \rightarrow \Lambda \bar{\Lambda}$ events and with a somewhat different set of systematic errors.

2.4 Future prospects

The eqn. 16 limit, $|\xi_P - \xi_S| < 0.94^\circ$ leaves considerable room for the influence of possible new physics in Ξ hyperon decay processes to appear before the expected level SM \mathcal{CP} violations is reached. The most recent calculation of the SM values for the ξ_P and ξ_S \mathcal{CP} -violating phases found their difference to be [40]

$$(\xi_P - \xi_S)_{\text{SM}} = -(1.4 \pm 1.2) A^2 \lambda^5 \bar{\eta} = -0.01^\circ \pm 0.01^\circ, \quad (21)$$

where $A^2 \lambda^5 \bar{\eta}$ is the imaginary part of the $V_{td}^* V_{ts}$ CKM matrix element product in the Wolfenstein parameterization [51]. This is a factor of a hundred below the statistical precision of the above-described BESIII measurement.

But not the systematic error, which is only ten times the SM value for $\xi_P - \xi_S$, despite the fact that \mathcal{CP} studies were not considered during the design of the general-purpose BESIII detector. This reflects the above-mentioned features of the $J/\psi \rightarrow \Xi \bar{\Xi}$ events that make them a robust platform for \mathcal{CP} violation studies. A detector at a future facility could be more closely tailored to the requirements of \mathcal{CP} studies, and, since BESIII's quoted 0.1° systematic errors are, for the most part, statistical errors associated with the numbers of control sample events that were used for their evaluation, these would be smaller for larger J/ψ event samples. Thus, it seems reasonable to expect that a specialized facility capable of producing and handling multi-trillion J/ψ event samples could have an $\xi_P - \xi_S$ measurement sensitivity that is near the 0.01° SM level.

3 Tests of the \mathcal{CPT} invariance with J/ψ decays

The \mathcal{CPT} theorem [52] states that any quantum field theory that is *Lorentz invariant*, has *local point-like interaction vertices*, and is *hermitian* (i.e., conserves probability) is invariant under the combined operations of \mathcal{C} , \mathcal{P} and \mathcal{T} . Since the three quantum field theories that make up the Standard Model—QED, QCD, and Electroweak theory—all satisfy these criteria, \mathcal{CPT} symmetry is a fundamental and inescapable prediction of

the theory. Any deviation from \mathcal{CPT} invariance would be unambiguous evidence for new, beyond the Standard Model physics. Given the central role that the \mathcal{CPT} theorem plays in our understanding of the most basic properties of space and time, it is essential that its validity should be tested at the highest level of sensitivity that experimental technology permits.

Fortunately, the K^0 - \bar{K}^0 mixing process coupled with the requirements of unitarity provide sensitive ways to search for violations of the \mathcal{CPT} theorem. This is embodied in a remarkable equation called the *Bell-Steinberger relation* that unambiguously relates a fundamental \mathcal{CPT} violating amplitude called δ to well defined measurable quantities. The relation is exact and, unlike most other experimental tests of the Standard Model, there are no loose ends such as long-distance QCD-corrections or theoretical assumptions about anything other than unitarity and time independence of the Hamiltonian. If a nonzero value of δ is established, the only possible interpretations are that either the \mathcal{CPT} theorem is invalid, or unitarity is violated, or that kaon mass or lifetime changes with time.

The measurement involves studies of the proper-time-dependence of the decay rates of large numbers of neutral kaons that have well established (*i.e.*, *tagged*) strangeness quantum numbers at the time of their production $K^0(\tau)$ for $S=+1$ and $\bar{K}^0(\tau)$ for $S=-1$. The most sensitive limits to date are from experiments in the 1990s that used data samples that contained tens of millions of K^0 and \bar{K}^0 decays. A $\sim 10^{12}$ -event sample of J/ψ decays will contain ~ 2 B $J/\psi \rightarrow K^- \pi^+ K^0$ events and an equivalent number of $J/\psi \rightarrow K^+ \pi^- \bar{K}^0$ events where the neutral kaon decays to $\pi^+ \pi^-$, and ~ 1 B events for each mode in which the kaon decays to $\pi^0 \pi^0$. In these reactions, the initial strangeness of the neutral kaon is tagged by the sign of the accompanying charged-kaon's electric charge: a K^- tags an $S=+1$ $K^0(\tau)$ and a K^+ tags an $S=-1$ $\bar{K}^0(\tau)$. These data samples would support a repeat of previous measurements with \sim fifty-times larger data samples.

In this talk I discuss:

- i) why we expect \mathcal{CPT} to be violated somewhere below the Planck mass-scale;
- ii) why the neutral kaon system is well suited for tests of the \mathcal{CPT} theorem;
- iii) the quantum-mechanics of neutral kaons with restrictions on \mathcal{CPT} relaxed;
- iv) estimated experimental sensitivities with 10^{12} J/ψ decays;
- v) applications of the Bell-Steinberger relation at a specialized J/ψ facility.

3.1 \mathcal{CPT} and the Theory of Everything

One of the requirements for a \mathcal{CPT} -invariant theory is that it is *local*, which means that the couplings at each vertex occurs at a single point in space-time. But theoretical physics has always had troubles with point-like quantities. For example, the classical Coulombic self-energy of the electron is

$$W_e = \frac{e^2}{4\pi\epsilon_0 r_e}, \quad (22)$$

which diverges for $r_e \rightarrow 0$. The *classical radius of the electron*, *i.e.*, the value of r_e that makes $W_e = m_e c^2$, is $r_e^{c.r.e.} = 2.8 \times 10^{-13}$ cm (2.8 fermis), which is three times the radius of the proton, and ~ 3000 times larger than the experimental upper limit on the electron radius, which is of $\mathcal{O}(10^{-16}$ cm) [53]. Infinities associated with point-like objects persist in quantum field theories, where they are especially troublesome. In second-

and higher-order perturbation theory, all of the diagrams that have virtual-particle loops involve integrals over all possible configurations of the loops that conserve energy and momentum. Whenever two of the point-like vertices coincide, the integrands become infinite and cause the integrals to diverge.

In the QED, QCD and Electroweak quantum field theories that make up the Standard Model, these infinities are removed by the well established methods of renormalization [54, 55, 56], a technique that involves the subtraction of two divergent quantities—where one of the divergences is associated with an established observable (like the free electron charge, or mass)—to produce a finite result. In all three of these theories, the perturbation expansions are in increasing powers of a dimensionless coupling strength, $\alpha_{\text{EW}} = \sqrt{2}M_W^2 G_F / \pi$,⁸ α_{QED} , and α_s . As a result of this, relations that exist between different orders of the perturbation expansion reduce the number of observed quantities that are needed to subtract off divergences. In QED, for example, there are only two, the electron’s mass, and charge. However, in quantum theories of gravity, where a massless spin=2 *graviton* plays the role of the photon in QED, the expansion constant is Newton’s gravitational constant with units $\text{m}^3/\text{kg}\cdot\text{s}^2$. Because of this, every order in the perturbation expansion has different dimensions and, thus, needs different observables to carry out the subtractions at each step. Thus a complete renormalization would require an infinite number of observed quantities to complete the renormalization, with the end effect that a quantum theory of gravity with point-like vertices would, in principle, be *non-renormalizable*[57]. As a result, a viable theory of everything will have to include a mechanism for avoiding these divergences by smearing out the vertices, for example by treating particles as loops of string as in Fig. 8, and this *non-locality* would eliminate one of the necessary conditions for \mathcal{CPT} invariance. In such a scenario, the Theory of Everything, which, by definition, would have to include gravity,⁹ would not be local and include \mathcal{CPT} violations at some mass scale.

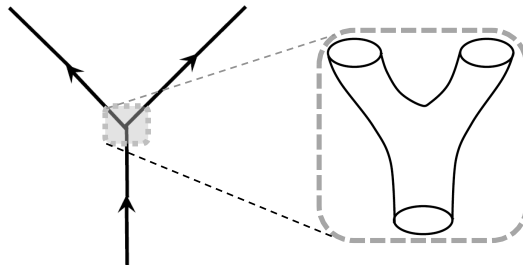


Figure 8: In string theories, elementary particles are tiny loops of oscillating strings with no point-like vertices and their associated infinities.

Although non-renormalizable higher-order perturbative effects do not show up at mass scales below the Planck mass ($M_P = \sqrt{\hbar c / G_N} = 1.22 \times 10^{19} \text{GeV}$), the fact that this problem exists dispels the notion that there is something especially sacred about \mathcal{CPT} -invariance; there is no fundamental principle that prevents it from being violated at a lower mass scale. Because of its close connection with the fundamental assumptions of the Standard Model, stringent experimental tests of \mathcal{CPT} invariance should have high priority

⁸Specifically not just G_F , which has dimensions of mass^{-2} .

⁹Even cavemen were aware of gravity.

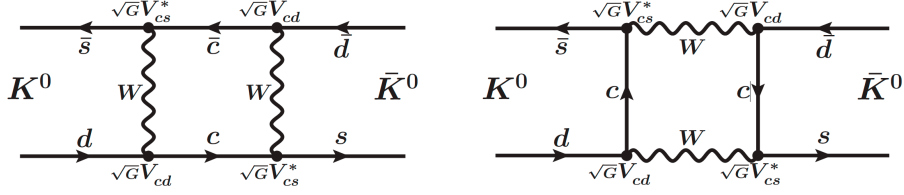


Figure 9: The box diagrams for the short-distance contributions to K^0 - \bar{K}^0 mixing.

3.2 Neutral K mesons and tests of the $\mathcal{CP}\mathcal{T}$ theorem

The main consequences of $\mathcal{CP}\mathcal{T}$ symmetry are that particle and antiparticle masses and lifetimes are equal. Since lifetime differences can only come from on-mass-shell intermediate states and do not probe short-distance high-mass physics, these are unlikely to exhibit any $\mathcal{CP}\mathcal{T}$ -violating asymmetry. Instead, our focus here is on the possibility that particle and antiparticle masses may be different.

The particles with the best measured masses are the stable electron and proton, and, according the PDG 2020 tables [58]:

$$|m_{e^+} - m_{e^-}| < 4 \times 10^{-9} \text{ MeV} \quad (23)$$

$$|m_{\bar{p}} - m_p| < 7 \times 10^{-7} \text{ MeV}. \quad (24)$$

However, these limits do not provide the best tests of $\mathcal{CP}\mathcal{T}$; the most stringent experimental restriction on $\mathcal{CP}\mathcal{T}$ violation comes from the difference between the \bar{K}^0 and K^0 masses:

$$|M_{\bar{K}^0} - M_{K^0}| < 5 \times 10^{-16} \text{ MeV}, \quad (25)$$

which is 7-9 orders of magnitude more strict than those from the electron and proton mass measurements, even though the value of M_{K^0} itself is only known to ± 13 keV. This is because the Fig. 9 diagrams, taken together with the quantum mechanics of K^0 - \bar{K}^0 mixing, map the $M_{\bar{K}^0} - M_{K^0}$ difference into the quantities $\Delta M = M_{K_L} - M_{K_S}$, which is 3.5×10^{-12} MeV and 14 orders of magnitude lower than $M_{\bar{K}^0}$ or M_{K^0} , and $\Delta\Gamma = \Gamma_{K_S} - \Gamma_{K_L} \approx 7.4 \times 10^{-12}$ MeV, which is, coincidentally, $\approx 2 \times \Delta M$.

3.3 The neutral kaon mass eigenstates with no $\mathcal{CP}\mathcal{T}$ -invariance related restrictions

Any arbitrary neutral kaon state in its rest frame can be expressed as a linear combination of the strangeness eigenstates, $|\psi\rangle = \alpha_1(\tau) |K^0\rangle + \alpha_2(\tau) |\bar{K}^0\rangle$, where $\alpha_1(\tau)$ and $\alpha_2(\tau)$ are complex functions that are normalized as $|\alpha_1(0)|^2 + |\alpha_2(0)|^2 = 1$. In the Wigner-Weisskopf formulation of quantum mechanics for exponentially decaying systems, the time dependence is included by using $\alpha_i(\tau) = \alpha_i^k e^{-i\lambda_k\tau}$ where α_i^k are complex constants and the Schrödinger equation in the form

$$\mathcal{H}\psi(\tau) = \left(\mathcal{M} - \frac{i}{2}\Gamma\right)\Psi_k e^{-i\lambda_k\tau} = i\frac{d\psi_K}{d\tau} = \lambda_k\Psi_k e^{-i\lambda_k\tau}, \quad (26)$$

where the Hamiltonian \mathcal{H} , the mass matrix \mathcal{M} and the decay matrix Γ are 2×2 matrices and Ψ_k is a two-dimensional spinor in (K^0, \bar{K}^0) space:

$$\mathcal{M} = \begin{pmatrix} M_{11} & M_{12} \\ M_{12}^* & M_{22} \end{pmatrix}, \quad \Gamma = \begin{pmatrix} \Gamma_{11} & \Gamma_{12} \\ \Gamma_{12}^* & \Gamma_{22} \end{pmatrix} \quad \text{and} \quad \Psi_k = \begin{pmatrix} \alpha_1^k \\ \alpha_2^k \end{pmatrix}. \quad (27)$$

Here \mathcal{M} and Γ are hermitian, which is ensured by setting $M_{21} = M_{12}^*$ and $\Gamma_{21} = \Gamma_{12}^*$, while \mathcal{H} , which describes decaying particles and doesn't conserve probability, is not hermitian. Symmetry under \mathcal{CP} requires M_{12} to be real; \mathcal{CPT} invariance requires $M_{11} = M_{22}$ and $\Gamma_{11} = \Gamma_{22}$. The mass eigenvalues and eigenstates for the most general case, *i.e.*, with neither \mathcal{CP} nor \mathcal{CPT} symmetry are [59, 60]

$$\begin{aligned}\lambda_S &= M_S - \frac{i}{\sqrt{2}}\Gamma_S; & |K_S\rangle &= \frac{1}{\sqrt{2(1+|\varepsilon_S|^2)}} \left[(1 + \varepsilon_S) |K^0\rangle + (1 - \varepsilon_S) |\bar{K}^0\rangle \right] \\ \lambda_L &= M_L - \frac{i}{\sqrt{2}}\Gamma_L; & |K_L\rangle &= \frac{1}{\sqrt{2(1+|\varepsilon_L|^2)}} \left[(1 + \varepsilon_L) |K^0\rangle - (1 - \varepsilon_L) |\bar{K}^0\rangle \right],\end{aligned}\quad (28)$$

where $\varepsilon_S = \varepsilon + \delta$, $\varepsilon_L = \varepsilon - \delta$ and ε & δ can be expressed in terms of $\Delta M \equiv M_L - M_S$ and $\Delta\Gamma \equiv \Gamma_S - \Gamma_L$ as

$$\varepsilon = \frac{-i \operatorname{Im} M_{12} - \frac{1}{2} \operatorname{Im} \Gamma_{12}}{\Delta M + \frac{i}{2} \Delta\Gamma}, \quad (29)$$

which is the familiar neutral kaon mass-matrix \mathcal{CP} violation parameter, and

$$\delta = \frac{(M_{\bar{K}^0} - M_{K^0}) - i(\Gamma_{\bar{K}^0} - \Gamma_{K^0})/2}{2\Delta M - i\Delta\Gamma}, \quad (30)$$

is the equivalent dimensionless parameter that characterizes mass-matrix \mathcal{CPT} violation parameter. A unique and important feature of this scenario is that the K_L and K_S eigenstates are not orthogonal; according to eqn. 28,

$$\langle K_S | K_L \rangle = 2 \operatorname{Re} \varepsilon - 2i \operatorname{Im} \delta, \quad (31)$$

where here, and in (most of) the following, second-order terms in $|\varepsilon|$ are dropped.

3.3.1 Properties of ε and δ

In a commonly used phase convention, $\operatorname{Im} \Gamma_{12}$ is defined to be zero, in which case the phase of ε is directly related to the well measured quantities¹⁰ ΔM and $\Delta\Gamma$ via

$$\phi_{\text{SW}} = \tan^{-1} \left(\frac{2\Delta M}{\Delta\Gamma} \right) = 43.5^\circ \pm 0.1^\circ, \quad \leftarrow \text{the Superweak phase} \quad (32)$$

that, since $\Delta M \approx \Delta\Gamma/2$, is very nearly 45° . Using this approximate relation for ϕ_{SW} , we can rewrite the eqn. 30 expression for δ as

$$\delta \approx \frac{i(M_{\bar{K}^0} - M_{K^0}) + (\Gamma_{\bar{K}^0} - \Gamma_{K^0})/2}{2\sqrt{2}\Delta M} e^{i\phi_{\text{SW}}} = (i\delta_\perp + \delta_\parallel) e^{i\phi_{\text{SW}}} \quad (33)$$

where the real quantities δ_\perp and δ_\parallel are defined as

$$\delta_\perp \approx \frac{M_{\bar{K}^0} - M_{K^0}}{2\sqrt{2}\Delta M} \quad \text{and} \quad \delta_\parallel = \frac{(\Gamma_{\bar{K}^0} - \Gamma_{K^0})}{4\sqrt{2}\Delta M}. \quad (34)$$

In the complex plane, δ_\perp , which is the short-distance component of δ , is perpendicular to ε , and δ_\parallel , the long-distance component, is parallel to ε . Thus, a signature for a nonzero short-distance \mathcal{CPT} violation would be a difference between the phase of ε_L and ϕ_{SW} by an amount

$$\Delta\phi^{\mathcal{CPT}} = \phi_{\varepsilon_L} - \phi_{\text{SW}} = \frac{\delta_\perp}{|\varepsilon|}, \quad (35)$$

¹⁰We use [61] $\Delta M = (0.5289 \pm 0.0010) \times 10^{10} \text{s}^{-1}$ & $\Delta\Gamma = (1.1149 \pm 0.0005) \times 10^{-10} \text{s}^{-1}$.

which means that

$$\begin{aligned} M_{\bar{K}^0} - M_{K^0} &= 2\sqrt{2}|\varepsilon|\Delta M\Delta\phi^{\mathcal{CP}\mathcal{T}} \\ &= 3.8 \times 10^{-16}(\text{MeV/deg}) \times \Delta\phi^{\mathcal{CP}\mathcal{T}}. \end{aligned} \quad (36)$$

The tiny proportionality constant between the $\mathcal{CP}\mathcal{T}$ -violating K^0 - \bar{K}^0 mass difference and the $\Delta\phi^{\mathcal{CP}\mathcal{T}}$ observable quantity is the reason the eqn.25 limit on $M_{\bar{K}^0} - M_{K^0}$ is many orders of magnitude more stringent than those for $m_{\bar{p}} - m_p$ (eqn.24) and $m_{\bar{e}} - m_e$ (eqn.23). This is the ‘‘magic’’ of the neutral kaon system and doesn’t apply to any other particles.

3.4 Interference measurements of the ϕ_{+-} and ϕ_{00} phases

A simulated $J/\psi \rightarrow K^- \pi^+ K^0(\tau); K^0(\tau) \rightarrow \pi^+ \pi^-$ event in the BESIII detector is shown in Fig. 10a. Although it looks superficially like a $K^- \pi^+ K_S$ event, the neutral kaon is not a K_S mass eigenstate and does not have a simple exponential decay curve. Instead, the neutral kaons produced in these reactions are coherent mixtures of interfering $|K_S\rangle$ and $|K_L\rangle$ eigenstates:

$$\begin{aligned} |K^0(\tau)\rangle &= \frac{1}{\sqrt{2}}[(1 + \varepsilon_L)|K_S\rangle e^{-i\lambda_S\tau} + (1 + \varepsilon_S)|K_L\rangle e^{-i\lambda_L\tau}] \\ |\bar{K}^0(\tau)\rangle &= \frac{1}{\sqrt{2}}[(1 - \varepsilon_L)|K_S\rangle e^{-i\lambda_S\tau} - (1 - \varepsilon_S)|K_L\rangle e^{-i\lambda_L\tau}], \end{aligned} \quad (37)$$

and have decay curves with opposite-sign K_S - K_L interference terms:

$$\left[\frac{R(\tau)_{K^0 \rightarrow \pi\pi}}{\bar{R}(\tau)_{\bar{K}^0 \rightarrow \pi\pi}} \right] \propto (1 \mp 2 \text{Re } \varepsilon_L) [e^{-\Gamma_S\tau} + |\eta_j|^2 e^{-\Gamma_L\tau} \pm 2|\eta_j| e^{-\bar{\Gamma}\tau} \cos(\Delta M\tau - \phi_j)],$$

where $\bar{\Gamma} = (\Gamma_S + \Gamma_L)/2 \approx \Gamma_S/2$ and $|\eta_j|$ and ϕ_j are the magnitudes and phases of η_{+-} and η_{00} :

$$\eta_{+-} = \frac{\langle \pi^+ \pi^- | K_L \rangle}{\langle \pi^+ \pi^- | K_S \rangle} = \varepsilon - \delta + \varepsilon' \quad \text{and} \quad \eta_{00} = \frac{\langle \pi^0 \pi^0 | K_L \rangle}{\langle \pi^0 \pi^0 | K_S \rangle} = \varepsilon - \delta - 2\varepsilon'. \quad (38)$$

Here $\varepsilon' = \langle \pi\pi | K_2 \rangle / \langle \pi\pi | K_1 \rangle$ is the ratio of the direct- \mathcal{CP} -violating amplitude of the \mathcal{CP} -odd $|K_2\rangle = \sqrt{\frac{1}{2}}(|K^0\rangle - |\bar{K}^0\rangle)$ eigenstate to \mathcal{CP} -even $\pi\pi$ final states to that for the

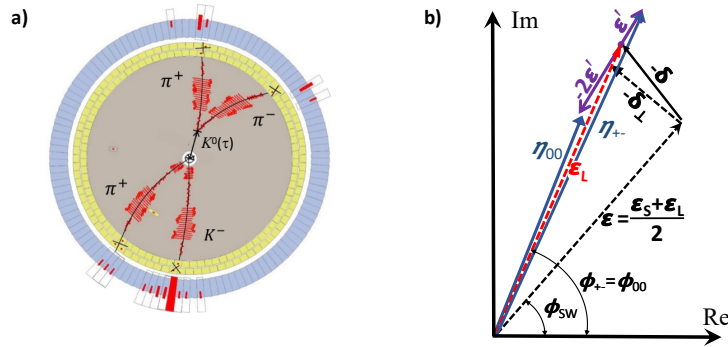


Figure 10: **a)** A simulated $J/\psi \rightarrow K^- \pi^+ K^0(\tau); K^0(\tau) \rightarrow \pi^+ \pi^-$ event in the BESIII detector. **b)** The relative arrangements on the complex plane of of the complex quantities discussed in the text. Here, for display purposes, the magnitudes of δ and ε' relative to ε are exaggerated.

\mathcal{CP} -allowed $\pi\pi$ decays of its \mathcal{CP} -even counterpart: $|K_1\rangle = \sqrt{\frac{1}{2}}(|K^0\rangle + |\bar{K}^0\rangle)$. Measurements [62, 63] have established that ε' is much smaller than ε :

$$\text{Re}(\varepsilon'/\varepsilon) = (1.66 \pm 0.23) \times 10^{-3}, \quad (39)$$

and its phase is determined from the analysis of low-energy $\pi\pi$ scattering measurements to be $\phi_{\varepsilon'} = 42.3^\circ \pm 1.7^\circ$ [64] and equal, within errors, to ϕ_{SW} . This rather remarkable coincidence¹¹ means that ε' and ε are very nearly parallel, and the combined effect of this with its small magnitude reduces the impact of the uncertainty of the magnitude of ε' on $\delta\phi^{\mathcal{CP}\mathcal{T}}$ measurements to negligible, $\mathcal{O}(0.01^\circ)$, levels. The arrangement of the various quantities discussed above on the complex plane is indicated in Fig. 10b.

3.4.1 Estimated measurement sensitivity with 10^{12} J/ψ -decays

Decay curves for $K^0(\tau) \rightarrow \pi^+\pi^-$ and $\bar{K}^0(\tau) \rightarrow \pi^+\pi^-$ for simulated BESIII events that were generated with PDG values of the η_{+-} magnitude and phase [65] are shown in Fig. 11a, where there are strong interference effects between the steeply falling $K_S \rightarrow \pi^+\pi^-$ and nearly flat $K_L \rightarrow \pi^+\pi^-$ amplitudes that have opposite signs for $K^0(\tau)$ - and $\bar{K}^0(\tau)$ -tagged decays. The difference between the interference terms is displayed in a plot of the reduced asymmetry [66] $\mathcal{A}'_{\pi\pi}$, where¹²

$$\begin{aligned} \mathcal{A}'_{\pi\pi} &\equiv \frac{\bar{N}(\bar{K}^0(\tau)) - N(K^0(\tau))}{\bar{N}(\bar{K}^0(\tau)) + N(K^0(\tau))} e^{-\frac{1}{2}\Delta\Gamma\tau} \\ &= 2 \text{Re} \varepsilon_L e^{-\frac{1}{2}\Delta\Gamma\tau} - 2 \frac{|\eta_j| \cos(\Delta M\tau - \phi_j)}{1 + |\eta_{+-}|^2 e^{\Delta\Gamma\tau}}, \end{aligned} \quad (40)$$

and is shown for the simulated data in Fig. 11b, where ϕ_j shows up as a phase shift in the interference-generated cosine-like oscillation.

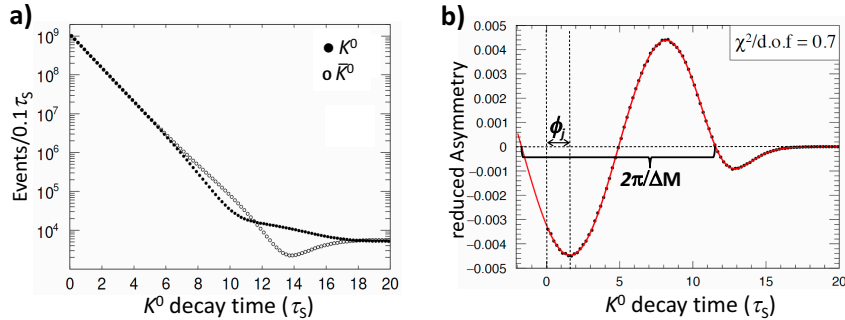


Figure 11: **a)** The solid circles show the proper time distribution for simulated strangeness-tagged $K^0(\tau) \rightarrow \pi^+\pi^-$ decays (the open circles are $\bar{K}^0(\tau) \rightarrow \pi^+\pi^-$ decays). **b)** The reduced asymmetry, $\mathcal{A}'_{\pi^+\pi^-}$, for the events shown in panel **a** (from ref. [65]).

The simulated data shown in Figs. 11 a & b correspond to 3.8B tagged $K \rightarrow \pi^+\pi^-$ decays that are almost equally split between $J/\psi \rightarrow \bar{K}^-\pi^+K^0$ and $J/\psi \rightarrow K^+\pi^-\bar{K}^0$

¹¹ $\phi_{\varepsilon'}$ is a long-distance QCD effect while ϕ_{SW} is due to short-distance EW physics.

¹² In the unmodified asymmetry, $\mathcal{A}_{\pi\pi} = [\bar{N}(\bar{K}^0(\tau)) - N(K^0(\tau))] / [\bar{N}(\bar{K}^0(\tau)) + N(K^0(\tau))]$, the $\cos(\Delta M\tau - \phi_j)$ oscillation term is multiplied by a factor $e^{\frac{1}{2}\Delta\Gamma\tau}$ that, when displayed, emphasizes low-statistics, long-decay-time events that, in fact, have little influence on the ϕ_j determination.

that were generated with $\Delta\phi^{\mathcal{CPT}}=0$ and $\phi_{\text{SW}}=43.5^\circ$. This corresponds to what one would expect for a total of 10^{12} J/ψ decays in a detector with realistic vertex and momentum resolutions that covered a $|\cos\theta| \leq 0.85$ solid angle. The red curve in the figure is the result of a fit to the data that determined [65]

$$\phi_{\text{SW}} + \Delta\phi^{\mathcal{CPT}} = 43.51^\circ \pm 0.05^\circ, \quad (41)$$

where the errors are statistical only. According to eqn. 36, this $\mathcal{O}(0.1^\circ)$ precision would correspond to $|M_{\bar{K}^0} - M_{K^0}| \approx 4 \times 10^{-17}$ MeV.

This would be an order of magnitude improvement over the existing eqn. 36 limit that is based on a 1995 result from Fermilab experiment E773 that used ~ 2 M $K \rightarrow \pi^+\pi^-$ and ~ 0.5 M $K \rightarrow \pi^0\pi^0$ decays produced downstream of a regenerator located in a high-energy K_L beam [67], and a 1999 result from the CPLEAR experiment at CERN [66] that used ~ 35 M-event samples of tagged $K^0(\tau) \rightarrow \pi^+\pi^-$ and $\bar{K}^0(\tau) \rightarrow \pi^+\pi^-$ decays produced via the annihilation of stopped antiprotons in a high-pressure gas hydrogen target into $K^\mp\pi^\pm K^0(\bar{K}^0)$ final states:

$$\begin{aligned} \text{E773 : } \quad \phi_{\text{SW}} + \Delta\phi^{\mathcal{CPT}} &= 42.94^\circ \pm 0.58^\circ(\text{stat}) \pm 0.49^\circ(\text{syst}) \\ \text{CPLEAR : } \quad \phi_{\text{SW}} + \Delta\phi^{\mathcal{CPT}} &= 42.91^\circ \pm 0.53^\circ(\text{stat}) \pm 0.28^\circ(\text{syst}). \end{aligned} \quad (42)$$

The CPLEAR systematic error includes a 0.19° component associated with the effects of regeneration in the high-pressure hydrogen gas in the stopping target and the walls of its containment vessel. In the E773 measurement, the phase off-set that was introduced by the regenerator was unavoidable and large, $\phi_{\text{regen}} \sim -130^\circ$, and was evaluated from a dispersion relation with an assigned error of 0.35° [68]. In an e^+e^- collider operating at the J/ψ with a detector optimized for \mathcal{CP} searches in hyperon decays and \mathcal{CPT} tests, the production and a significant fraction of the $K \rightarrow \pi^+\pi^-$ decays would occur in a vacuum, and the effects of regeneration on decays that occur outside the vacuum could be measured in specially configured data runs, as was done, *e.g.*, by the CPLEAR group [69]).

3.5 The Bell Steinberger relation

The above discussion is not entirely rigorous and ignores some corrections¹³ that are small compared to the precision of the KTeV and CPLEAR measurements in eqn. 42 but will be important for future measurements. For these, a procedure devised by John Bell and Jack Steinberger that gives an exact expression for $\text{Im } \delta$ in terms of measurable quantities and is phase-convention independent should be used [70].

As mentioned above, a general solution to the Schrödinger equation is given by

$$\psi(\tau) = \alpha_1 e^{-i\lambda_S \tau} |K_S\rangle + \alpha_2 e^{-i\lambda_L \tau} |K_L\rangle, \quad (43)$$

where α_1 and α_2 can be any complex constants subject only to the normalization condition $|\alpha_1|^2 + |\alpha_2|^2 = 1$. The time-dependent probability associated with this wave function is

$$|\psi(\tau)|^2 = |\alpha_1|^2 e^{-\Gamma_S \tau} + |\alpha_2|^2 e^{-\Gamma_L \tau} + 2 \text{Re} \left(\alpha_1^* \alpha_2 e^{-\frac{1}{2}(\Gamma_S + \Gamma_L + 2i\Delta M)\tau} \langle K_S | K_L \rangle \right), \quad (44)$$

¹³These are associated with ignoring the term involving $\text{Im } \Gamma_{12}$ in eqn. 29.

and the negative of its derivative at $\tau=0$ is

$$-\left. \frac{d|\psi(\tau)|^2}{d\tau} \right|_{\tau=0} = |\alpha_1|^2 \Gamma_S + |\alpha_2|^2 \Gamma_L + \text{Re} (\alpha_1^* \alpha_2 (\Gamma_S + \Gamma_L + 2i\Delta M) \langle K_S | K_L \rangle). \quad (45)$$

In the Weisskopf-Wigner formalism, the Schrödinger equation is not hermitian and the solutions do not conserve probability. Instead, the overall normalization has a time dependence given by

$$|\psi(\tau)|^2 = |\psi(0)|^2 e^{-\Gamma_{\text{tot}}\tau}; \quad \frac{d|\psi(\tau)|^2}{d\tau} = -\Gamma_{\text{tot}} e^{-\Gamma_{\text{tot}}\tau}, \quad (46)$$

and unitarity requires that

$$-\left. \frac{d|\psi(\tau)|^2}{d\tau} \right|_{\tau=0} = \Gamma_{\text{tot}} = \sum_j \Gamma_j = \sum_j |\langle f_j | \psi(0) \rangle|^2, \quad (47)$$

where the summation index j runs over all of the accessible final states $|f_j\rangle$. Applying this unitarity condition to the eqn. 43 wave function gives an independent expression for the derivative of $|\psi(\tau)|^2$ at $\tau=0$:

$$-\left. \frac{d|\psi(\tau)|^2}{d\tau} \right|_{\tau=0} = \sum_j |\alpha_1|^2 |\langle f_j | K_S \rangle|^2 + |\alpha_2|^2 |\langle f_j | K_L \rangle|^2 + 2 \text{Re} (\alpha_1^* \alpha_2 \langle f_j | K_S \rangle^* \langle f_j | K_L \rangle). \quad (48)$$

Equations 45 and 48 have to apply for any values of α_1 and α_2 (subject to $|\alpha_1|^2 + |\alpha_2|^2 = 1$), and, thus, the terms multiplying $\alpha_1^* \alpha_2$ in each expression have to be equal

$$(\Gamma_S + \Gamma_L + 2i\Delta M) \langle K_S | K_L \rangle = 2 \sum_j \langle f_j | K_S \rangle^* \langle f_j | K_L \rangle, \quad (49)$$

that, together with eqn. 31, becomes

$$\frac{1}{2} \langle K_S | K_L \rangle = \frac{\text{Re } \varepsilon}{1 + |\varepsilon|^2} - i \text{Im } \delta = \frac{\sum_j \langle f_j | K_S \rangle^* \langle f_j | K_L \rangle}{\Gamma_S + \Gamma_L + 2i\Delta M}, \quad (50)$$

which is the *Bell-Steinberger relation*. Here the second-order term in $|\varepsilon|$ is retained because with it, the equation is exact. A nonzero value of $\text{Im } \delta$ could only occur if \mathcal{CPT} is violated, or if unitarity is invalid, or if the M_{ij} and/or Γ_{ij} elements of the Hamiltonian were time dependent.

Because of the small number of K_S decay modes, the sum on the right-hand side of this equation only contains a few terms and is manageable. In contrast, the neutral D - and B -mesons have hundreds of established decay modes and probably a similar number of modes that have yet to be detected, and any attempt to apply a Bell-Steinberger-like unitarity constraint would be a hopeless task.

A Bell-Steinberger-relation evaluation of $\text{Im } \delta$ and $\text{Re } \varepsilon$ by Giancarlo D'Ambrosio and Gino Isidori in collaboration with the KLOE group that used of all the latest relevant measurements was originally presented in 2006 [71] and recently updated in the PDG2020 review [72]. Their results are:

channel	$\langle f_j K_S \rangle^* \langle f_j K_L \rangle (10^{-5} \Gamma_S)$
$\pi^+ \pi^- (\gamma)$	$112.1 \pm 1.0 + i(106.1 \pm 1.0)$
$\pi^0 \pi^0$	$49.3 \pm 0.5 + i(47.1 \pm 0.5)$
$\pi^+ \pi^- \gamma_{E1}$	< 0.01
$\pi^+ \pi^- \pi^0$	$0.0 \pm 0.2 + i(0.0 \pm 0.2)$
$\pi^0 \pi^0 \pi^0$	< 0.15
$\pi^\pm \ell^\mp \nu$	$-0.1 \pm 0.2 + i(-0.1 \pm 0.5)$,

where: the $\pi\pi(\gamma)$ values come from the PDG 2020 averages of many η_{+-} and η_{00} measurements; the $\pi^+ \pi^- \gamma_{E1}$ limit comes from theory [73, 74]; the $\pi\pi\pi$ results are based on thirty-year-old $\mathcal{B}(K_S \rightarrow \pi^+ \pi^- \pi^0)$ measurements [75, 76] and a 2013 KLOE upper bound on $\mathcal{B}(K_S \rightarrow \pi^0 \pi^0 \pi^0)$ [77]; and the $\pi^\pm \ell^\mp \nu$ values come from twenty-five-year-old limits on $\Delta\mathcal{S} = -\Delta Q$ processes from CPLEAR [78].

The bottom line of this analysis is

$$\text{Im } \delta = (-0.3 \pm 1.4) \times 10^{-5} \Rightarrow |M_{\bar{K}^0} - M_{K^0}| < 4 \times 10^{-16} \text{ MeV}, \quad (51)$$

and the $\text{Im } \delta$ vs. $\text{Re } \varepsilon$ and $\Gamma_{\bar{K}^0} - \Gamma_{K^0}$ vs. $M_{\bar{K}^0} - M_{K^0}$ allowed regions are shown in Figs. 12 a & b, respectively. The limit on $|M_{\bar{K}^0} - M_{K^0}|$ is nearly the same as the eqn. 36 limit that comes from simply comparing the PDG 2020 world average values for ϕ_{+-} and ϕ_{SW} . This is not surprising since in both analyses the $\pi\pi$ channels dominate and the sensitivities are limited by the same η_{+-} and η_{00} measurement errors. Moreover the contributions from the three-body modes and their errors are smaller than those from the $\pi\pi$ modes. However, when compared to the projected errors of measurements with 10^{12} J/ψ events, the errors on these auxiliary contributions are not small, and, thus, future progress in Bell-Steinberger-relation analyses will require that improvements in the η_{+-} and η_{00} phase measurements are accompanied by similar improvements in the precision of the other terms.

The $\pi^+ \pi^- \pi^0$ entry in the above table are from statistics-limited time-dependent Dalitz-plot analyses of $K_S - K_L$ interference effects in strangeness-tagged $K^0(\tau)$ and $\bar{K}^0(\tau)$ decays to $\pi^+ \pi^- \pi^0$. Similarly, the $\pi\ell\nu$ entry is limited by the measured values lepton charge asymmetries that were used to establish limits on violations of the $\Delta\mathcal{S} = \Delta Q$ rule that also used strangeness-tagged kaons. The precision of both of these

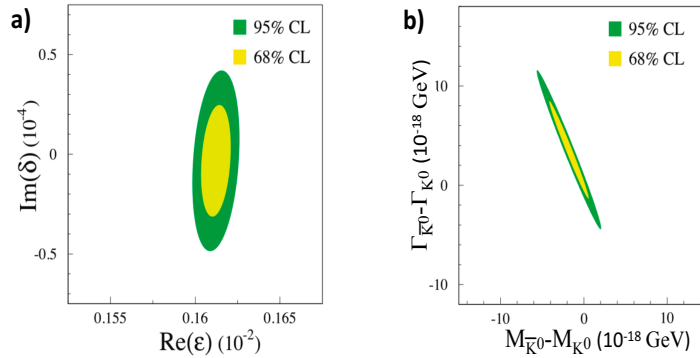


Figure 12: **a)** The 68% and 95% confidence level allowed region for $\text{Im } \delta$ and $\text{Re } \varepsilon$ from a Bell-Steinberger analysis. **b)** The corresponding allowed regions in $\Delta\Gamma = \Gamma_{\bar{K}^0} - \Gamma_{K^0}$ and $\Delta M = M_{\bar{K}^0} - M_{K^0}$. From ref. [58].

entries could be improved with the higher statistics data samples that would be available at a future facility.

That leaves the $\pi^0\pi^0\pi^0$ entry, which is not a limiting factor now, but will be if (or when) the $\pi^+\pi^-$ and $\pi^0\pi^0$ and other entries are improved by an order of magnitude. It is based on a $\mathcal{B}(K_S \rightarrow 3\pi^0) < 2.6 \times 10^{-8}$ upper limit.¹⁴ from the KLOE experiment that used tagged K_S mesons in a 1.7 billion $e^+e^- \rightarrow \phi \rightarrow K_S K_L$ event data sample produced at the DAFNE ϕ factory [77]. The KLOE analysis detected 75 M $K_S \rightarrow \pi^0\pi^0$ decays but found zero $K_S \rightarrow 3\pi^0$ events. In the absence of any prospects for a next-generation ϕ factory, further improvements of this entry will not be easy.

4 The strange history of the Standard Model

In the 1950s and 60s, measurements of the “strange” properties of the newly discovered hyperons and kaons taught us almost all of what was needed to develop the Standard Model, including:

Flavor Quantum Numbers: “Strangeness” was the first of the SM’s “flavors” to be identified;

Particle-antiparticle Mixing: $K^0 \leftrightarrow \bar{K}^0$ -like transitions also occur with charmed and bottom particles, and related processes occur with neutrinos;

Parity Violation: left-right symmetry violating processes were first seen in K -meson decays and are now a defining characteristic of the Weak Interactions;

\mathcal{CP} Violation: the first sign of matter and antimatter differences was the observation of $K_L \rightarrow \pi^+\pi^-$ decays;

Flavor mixing: the suppression of the $\Lambda \rightarrow pe^-\bar{\nu}$ decay rate below that inferred from the half-life for $n \rightarrow pe^-\bar{\nu}$ decay was the first sign of flavor-mixing, and the precursor of the CKM quark-mixing and PMNS neutrino-mixing matrices;

Quark Model: the Isospin-Strangeness patterns in the baryon octet & decuplet and the meson octets led to the discovery of $SU(3)$ and fractionally charged quarks;

Color: the existence of Ω^- baryon that, in the quark model, was comprised of three identical s -quarks in a symmetric state, indicated the existence of a hidden “color” quantum number;

GIM Mechanism: the strong suppression of strangeness-changing neutral-current kaon decays led to prediction of the existence of the c -quark;

Six quarks: the accommodation of \mathcal{CP} violation into quark-flavor-mixing matrix required a minimum of six quark flavors.

This all occurred before the 1974 discovery of the J/ψ . The only subsequent discovery that could not be accounted for by the Standard Model was neutrino mixing, which was predicted by Bruno Pontecorvo [79] in 1958, who was inspired by the 1955 discovery of K - \bar{K} mixing.

¹⁴The SM expectation is $\sim 10 \times$ lower at $\mathcal{B}^{\text{SM}}(K_S \rightarrow 3\pi^0) \approx |\epsilon|^2 (\tau_S / \tau_L) \mathcal{B}(K_L \rightarrow 3\pi^0) = 1.7 \times 10^{-9}$.

After the c -quark discovery, interest in strangeness physics abated and, after the 1990s, none the world's major particle physics developed the capability of producing enough kaons to match, much less improve on, the E773 and CPLEAR results, choosing instead to focus on experiments with huge numbers of charmed and beauty particles that can address many interesting subjects, but will never be able to test the \mathcal{CPT} theorem with the exquisite sensitivity that is uniquely provided by the neutral K -meson system or search for new sources of \mathcal{CP} violation in hyperon decay. As noted in this report, a facility that could produce $\sim 10^{12}$ J/ψ per year (or so) would provide opportunities to make order of magnitude sensitivity improvements over earlier experiments in both areas, all with relatively modest costs, especially for a laboratory with existing intense electron and positron sources.

Strange particles taught us a lot in the past, maybe they'll teach us even more in the future.

5 Acknowledgement

The author thanks the organizers and staff of the 50 Years Discovery of the J Particle Symposium for inviting me to give this talk and their kind hospitality during our visit to Beijing. I also acknowledge numerous informative discussions about the material contained in this report with my BESIII colleagues Andrzej Kupsc, Haibo Li, Jian-Yu Zhang and Xiaorong Zhou. This work was supported in part by the National Research Foundation of Korea under Contract No. NRF-2022R1A2C1092335, and the PIFI program of the Chinese Academy of Science.

A Appendix on monochromatic beams

A possible method to increase the J/ψ event rate without increasing beam currents and is specific to a $e^+e^- \rightarrow J/\psi$ c.m. collider, would involve decreasing the effective e^+e^- c.m. energy spread. In circular e^+e^- storage rings, statistical fluctuations in the number of synchrotron X-rays that are radiated turn-to-turn create an irreducible energy spread in the circulating e^+ and e^- beams that, in the BEPCII collider, is $\sigma_{\text{rms}}(E_{\text{beam}}) \approx 5 \times 10^{-4} E_{\text{beam}}$. Thus, although the J/ψ is a Breit Wigner resonance with a peak cross-section of $90 \mu\text{b}$ and a FWHM width¹⁵ of $\Gamma = 93 \text{ keV}$, as shown as a black curve in Fig. 13a, the c.m. energy spread in BESIII dilutes this narrow peak to a visible line-shape that is a Gaussian with a $\sigma_{\text{vis}}(e^+e^- \rightarrow J/\psi) = 3.4 \mu\text{b}$ peak cross-section with a 1.1 MeV rms energy spread, as shown by the blue curve in Fig. 13a. When the collider operates at the J/ψ mass peak, about 96% of the e^+e^- combinations have an energy sum that is either too low or too high to produce a J/ψ , as illustrated by the cartoon in the upper panel of Fig. 13b.

A monochromator scheme that was first proposed by Alfredo Renieri [80] and, independently, by Igor Protopopov, Alexander Skrinsky & Alexander Zholents [81], could improve the E_{cm} resolution with a commensurate increase in the visible J/ψ peak cross section. This would be accomplished by introducing some energy dispersion into both beams at their collision point, *i.e.*, a horizontal position dependence of the beam-particle energy, as shown in the lower portion of Fig. 13b. Here the dispersion is arranged so the low-energy side of the e^- beam collides with the high energy side of the e^+ beam profile, and *vice versa*, thereby reducing the effective c.m. energy

¹⁵The corresponding rms width is $\sigma_{\text{rms}} \approx 40 \text{ keV}$.

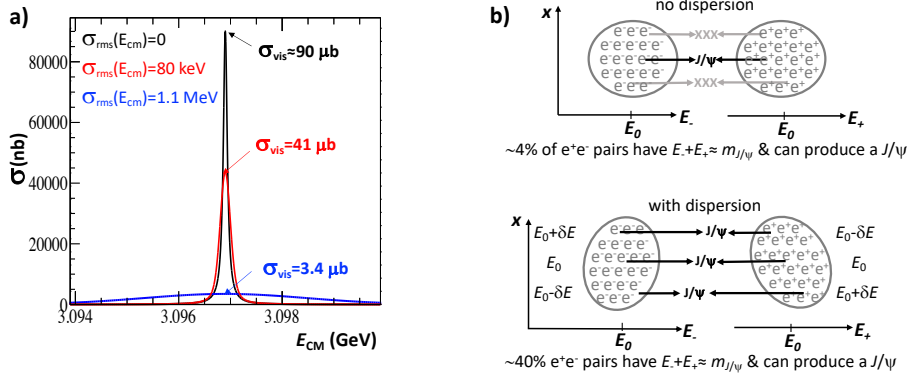


Figure 13: **a)** The visible $e^+e^- \rightarrow J/\psi$ lineshape for different values of the E_{cm} resolution (provided by Xiaoshuai Qin). **b)** Usually colliders operate with zero dispersion at the interaction point, with no correlation between a beam particle's energy and its horizontal position, as shown in the upper part of the figure. In monochromator operation, dispersion is introduced as shown in the lower section, so that lower energy particles in one beam preferentially collide with higher energy particles in the other beam (and *vice versa*).

spread. If $\sigma_{\text{rms}}(E_{\text{cm}})$ can be reduced to ≈ 80 keV, the peak cross section would be ten times higher at $\sigma_{\text{vis}}(e^+e^- \rightarrow J/\psi) \approx 41 \mu\text{b}$ as shown as a red curve in Fig. 13a. A lattice design by Zholents provided a proof of principle that an order of magnitude improvement in the E_{cm} resolution could be achieved in a head-on collider [82].

A variation of this technique to large-crossing-angle colliders that includes angular dispersion in addition to energy dispersion was proposed by Valery Telnov [83]. He concludes that an e^+e^- collider operating with a very large crossing angle, ~ 300 mrad—four times SuperKEKB's 83 mrad crossing angle—could reduce the effective mass resolution by as much as two orders of magnitude, in which case the visible cross section at the J/ψ peak would be the full $90 \mu\text{b}$, with no apparent luminosity penalty. Although such a large crossing angle would be a major complication for a general purpose facility, where some physics goals might require hermetic 4π detector coverage and/or meticulous micro-vertex resolution, it would probably be tolerable for most J/ψ -related topics, including the above-described $\mathcal{CP}\mathcal{T}$ test.

References

- [1] J. Z. Bai et al. Structure analysis of the $f(J)$ (1710) in the radiative decay $J/\psi \rightarrow \gamma K^+ K^-$. *Phys. Rev. Lett.*, 77:3959–3962, 1996.
- [2] J. Z. Bai et al. Partial wave analysis of $J/\psi \rightarrow \gamma(\eta \pi^+ \pi^-)$. *Phys. Lett. B*, 446:356–362, 1999.
- [3] S. X. Nakamura, Q. Huang, J. J. Wu, H. P. Peng, Y. Zhang, and Y. C. Zhu. Three-body unitary coupled-channel approach to radiative J/ψ decays and $\eta(1405/1475)$. *Phys. Rev. D*, 109(1):014021, 2024.
- [4] N. N. Achasov, A. A. Kozhevnikov, and G. N. Shestakov. Isospin breaking decay $\eta(1405) \rightarrow f_0(980)\pi^0 \rightarrow 3\pi$. *Phys. Rev. D*, 92(3):036003, 2015.
- [5] M. Ablikim et al. The sigma pole in $J/\psi \rightarrow \omega \pi^+ \pi^-$. *Phys. Lett. B*, 598:149–158, 2004.

- [6] M. Ablikim et al. Evidence for kappa meson production in $J/\psi \rightarrow \text{anti-K}^*(892)0 K^+ \pi^-$ process. *Phys. Lett. B*, 633:681–690, 2006.
- [7] S. Navas et al. Review of particle physics. *Phys. Rev. D*, 110(3):030001, 2024.
- [8] J. Z. Bai et al. Observation of a near threshold enhancement in the p anti-p mass spectrum from radiative $J/\psi \rightarrow \gamma p \text{ anti-p}$ decays. *Phys. Rev. Lett.*, 91:022001, 2003.
- [9] M. Ablikim et al. Observation of a resonance X(1835) in $J/\psi \rightarrow \gamma \pi^+ \pi^- \eta'$. *Phys. Rev. Lett.*, 95:262001, 2005.
- [10] Gui-Jun Ding and Mu-Lin Yan. Productions of X(1835) as baryonium with sizable gluon content. *Eur. Phys. J. A*, 28:351–360, 2006.
- [11] Medina Ablikim et al. Observation of an anomalous line shape of the $\eta' \pi^+ \pi^-$ mass spectrum near the $p\bar{p}$ mass threshold in $J/\psi \rightarrow \gamma \eta' \pi^+ \pi^-$. *Phys. Rev. Lett.*, 117(4):042002, 2016.
- [12] M. Ablikim et al. Observation of an Isoscalar Resonance with Exotic $J^{PC}=1^{-+}$ Quantum Numbers in $J/\psi \rightarrow \gamma \eta \eta'$. *Phys. Rev. Lett.*, 129(19):192002, 2022. [Erratum: *Phys.Rev.Lett.* 130, 159901 (2023)].
- [13] A. Rodas et al. Determination of the pole position of the lightest hybrid meson candidate. *Phys. Rev. Lett.*, 122(4):042002, 2019.
- [14] Medina Ablikim et al. Determination of Spin-Parity Quantum Numbers of X(2370) as 0^{-+} from $J/\psi \rightarrow \gamma K^0 \bar{K}^0 \eta'$. *Phys. Rev. Lett.*, 132(18):181901, 2024.
- [15] M. Ablikim et al. Observation of $a_0^0(980)$ - $f_0(980)$ Mixing. *Phys. Rev. Lett.*, 121(2):022001, 2018.
- [16] Shuang-Shi Fang. Light meson physics at BESIII. *Natl. Sci. Rev.*, 8(11):nwab052, 2021.
- [17] N. N. Achasov, S. A. Devyanin, and G. N. Shestakov. The $S^* \Delta^0$ Mixing as the Threshold Phenomenon. *Phys. Lett. B*, 88:367–371, 1979.
- [18] Nikolai Nikolaevich Achasov and G. N. Shestakov. Strong isospin symmetry breaking in light scalar meson production. *Phys. Usp.*, 62(1):3–31, 2019.
- [19] Robert L. Jaffe. Multi-Quark Hadrons. 1. The Phenomenology of (2 Quark 2 anti-Quark) Mesons. *Phys. Rev. D*, 15:267, 1977.
- [20] V. A. Rubakov and M. E. Shaposhnikov. Electroweak baryon number nonconservation in the early universe and in high-energy collisions. *Usp. Fiz. Nauk*, 166:493–537, 1996.
- [21] A. Augusto Alves, Jr. et al. The LHCb Detector at the LHC. *JINST*, 3:S08005, 2008.
- [22] T. Aushev et al. Physics at Super B Factory. 2010. arXiv:1002.5012.
- [23] Gershon T. and Nir Y. CP Violation in the Quark Sector. *Phys. Rev. D*, 110(3):280, 2024. Review article in the PDG 2024 review.

- [24] Roel Aaij et al. Observation of charge-parity symmetry breaking in baryon decays. 3 2025.
- [25] Xiao-Gang He, Chia-Wei Liu, and Jusak Tandean. Large CP violation in $\Lambda_b^0 \rightarrow pK^-\pi^+\pi^-$ and its U-spin partner decays. 3 2025.
- [26] Yuval Grossman, Alexander L. Kagan, and Yosef Nir. New physics and CP violation in singly Cabibbo suppressed D decays. *Phys. Rev. D*, 75:036008, 2007.
- [27] R. Aaij et al. Evidence for CP violation in time-integrated $D^0 \rightarrow h^-h^+$ decay rates. *Phys. Rev. Lett.*, 108:111602, 2012.
- [28] Roel Aaij et al. Observation of CP Violation in Charm Decays. *Phys. Rev. Lett.*, 122(21):211803, 2019.
- [29] Hai-Yang Cheng and Cheng-Wei Chiang. SU(3) symmetry breaking and CP violation in D \rightarrow PP decays. *Phys. Rev. D*, 86:014014, 2012.
- [30] Yuval Grossman and Dean J. Robinson. SU(3) Sum Rules for Charm Decay. *JHEP*, 04:067, 2013.
- [31] C. Abel et al. Measurement of the Permanent Electric Dipole Moment of the Neutron. *Phys. Rev. Lett.*, 124(8):081803, 2020.
- [32] V. Andrew et al. Improved limit on the electric dipole moment of the electron. *Nature*, 562(7727):355–360, 2018.
- [33] Tanya S. Roussy et al. An improved bound on the electron’s electric dipole moment. *Science*, 381(6653):adg4084, 2023.
- [34] K. Abe et al. Hyper-Kamiokande Design Report. unpublished, 5 2018.
- [35] B. Abi et al. Long-baseline neutrino oscillation physics potential of the DUNE experiment. *Eur. Phys. J. C*, 80(10):978, 2020.
- [36] Sacha Davidson, Enrico Nardi, and Yosef Nir. Leptogenesis. *Phys. Rept.*, 466:105–177, 2008.
- [37] A. Lai et al. A Precise measurement of the direct CP violation parameter $\text{Re}(\epsilon'/\epsilon)$. *Eur. Phys. J. C*, 22:231–254, 2001.
- [38] A. Alavi-Harati et al. Observation of direct CP violation in $K_{S,L} \rightarrow \pi\pi$ decays. *Phys. Rev. Lett.*, 83:22–27, 1999.
- [39] Andrzej J. Buras. The ϵ'/ϵ -Story: 1976-2021. *Acta Phys. Polon. B*, 52(1):7–41, 2021.
- [40] Jusak Tandean and G. Valencia. CP violation in hyperon nonleptonic decays within the standard model. *Phys. Rev. D*, 67:056001, 2003.
- [41] Xiao-Gang He, Hitoshi Murayama, Sandip Pakvasa, and G. Valencia. CP violation in hyperon decays from supersymmetry. *Phys. Rev. D*, 61:071701, 2000. arXiv:hep-ph/9909562.
- [42] Elisabetta Perotti, Göran Fäldt, Andrzej Kupsc, Stefan Leupold, and Jiao Jiao Song. Polarization observables in e^+e^- annihilation to a baryon-antibaryon pair. *Phys. Rev. D*, 99(5):056008, 2019.

- [43] T. D. Lee, J. Steinberger, G. Feinberg, P. K. Kabir, and Chen-Ning Yang. Possible Detection of Parity Nonconservation in Hyperon Decay. *Phys. Rev.*, 106:1367–1369, 1957.
- [44] John F. Donoghue and Sandip Pakvasa. Signals of CP Nonconservation in Hyperon Decay. *Phys. Rev. Lett.*, 55:162, 1985.
- [45] Martin Hoferichter, Jacobo Ruiz de Elvira, Bastian Kubis, and Ulf-G. Meißner. Roy–Steiner-equation analysis of pion–nucleon scattering. *Phys. Rept.*, 625:1–88, 2016.
- [46] Bo-Lin Huang, Jin-Sheng Zhang, Yun-De Li, and Norbert Kaiser. Meson-baryon scattering to one-loop order in heavy baryon chiral perturbation theory. *Phys. Rev. D*, 96(1):016021, 2017.
- [47] Medina Ablikim et al. Probing CP symmetry and weak phases with entangled double-strange baryons. *Nature*, 606(7912):64–69, 2022.
- [48] Medina Ablikim et al. Tests of CP symmetry in entangled Ξ^0 - $\bar{\Xi}^0$ pairs. *Phys. Rev. D*, 108(3):L031106, 2023.
- [49] Medina Ablikim et al. Precise Measurement of Matter-Antimatter Asymmetry with Entangled Hyperon Antihyperon pairs. To be published, 2025.
- [50] M. Ablikim et al. Precision measurements of decay parameters and CP asymmetry in Λ decays. 4 2022. arXiv:2204.11058.
- [51] Lincoln Wolfenstein. Parametrization of the Kobayashi-Maskawa Matrix. *Phys. Rev. Lett.*, 51:1945, 1983. the PDG 2020 central values are $\eta = 0.355$, $A = 0.84$, & $\lambda = 0.2245$.
- [52] Julian S. Schwinger. The Theory of quantized fields. 1. *Phys. Rev.*, 82:914–927, 1951.
- [53] S. Chekanov et al. Search for contact interactions, large extra dimensions and finite quark radius in e p collisions at HERA. *Phys. Lett. B*, 591:23–41, 2004.
- [54] H. A. Bethe. The Electromagnetic shift of energy levels. *Phys. Rev.*, 72:339–341, 1947.
- [55] F. J. Dyson. The Radiation theories of Tomonaga, Schwinger, and Feynman. *Phys. Rev.*, 75:486–502, 1949.
- [56] K. G. Wilson and John B. Kogut. The Renormalization group and the epsilon expansion. *Phys. Rept.*, 12:75–199, 1974.
- [57] Steven Weinberg and Edward Witten. Limits on Massless Particles. *Phys. Lett. B*, 96:59–62, 1980.
- [58] P. A. Zyla et al. Review of Particle Physics. *PTEP*, 2020(8):083C01, 2020.
- [59] Ikaros I. Bigi and A. I. Sanda. *CP violation*, volume 9. Cambridge University Press, 9 2009.
- [60] Klaus R. Schubert. T Violation and CPT Tests in Neutral-Meson Systems. *Prog. Part. Nucl. Phys.*, 81:1–38, 2015.

- [61] R. L. Workman and Others. Review of Particle Physics. *PTEP*, 2022:083C01, 2022.
- [62] J. R. Batley et al. A Precision measurement of direct CP violation in the decay of neutral kaons into two pions. *Phys. Lett. B*, 544:97–112, 2002.
- [63] E. Abouzaid et al. Precise Measurements of Direct CP Violation, CPT Symmetry, and Other Parameters in the Neutral Kaon System. *Phys. Rev. D*, 83:092001, 2011. arXiv:1011.0127.
- [64] G. Colangelo, J. Gasser, and H. Leutwyler. $\pi\pi$ scattering. *Nucl. Phys. B*, 603:125–179, 2001.
- [65] Jian-Yu Zhang, Cheng-Dong Fu, Hai-Bo Li, Liang Liu, and Xiao-Rong Zhou. Measurement of CP violation of neutral kaon system in J/ψ decay at the Super Tau-Charm Facility. 9 2022.
- [66] A. Apostolakis et al. A Determination of the CP violation parameter η_{+-} from the decay of strangeness tagged neutral kaons. *Phys. Lett. B*, 458:545–552, 1999.
- [67] B. Schwingerheuer et al. CPT tests in the neutral kaon system. *Phys. Rev. Lett.*, 74:4376–4379, 1995.
- [68] Roy A. Briere and Bruce Winstein. Determining the phase of a strong scattering amplitude from its momentum dependence to better than 1-degree: The Example of Kaon regeneration. *Phys. Rev. Lett.*, 75:402–405, 1995. [Erratum: *Phys.Rev.Lett.* 75, 2070 (1995)].
- [69] A. Angelopoulos et al. Measurement of the neutral kaon regeneration amplitude in carbon at momenta below 1-GeV/c. *Phys. Lett. B*, 413:422–430, 1997.
- [70] J. S. Bell and J. Steinberger. Weak Interactions of Kaons. In *Proceedings of the Oxford Int. Conf. on Elementary Particles*, pages 195–222, 1965.
- [71] Giancarlo D’Ambrosio and Gino Isidori. Determination of CP and CPT violation parameters in the neutral kaon system using the Bell-Steinberger relation and data from the KLOE experiment. *JHEP*, 12:011, 2006.
- [72] M. Antonelli, G. D’Ambrosio, and M.S. Sozzi. *cpt* invariance testa in neutral kaon decay (pdg review article). *PTEP*, 2022:871, 2022.
- [73] Hai-Yang Cheng. Radiative kaon decays $K^{+-} \rightarrow \pi^{+-} \pi^0 \gamma$ and direct CP violation. *Phys. Rev. D*, 49:3771–3774, 1994.
- [74] Giancarlo D’Ambrosio and Gino Isidori. CP violation in kaon decays. *Int. J. Mod. Phys. A*, 13:1–94, 1998.
- [75] Y. Zou et al. New measurement of the amplitude of the CP conserving decay $K_S \rightarrow \pi^+ \pi^- \pi^0$. *Phys. Lett. B*, 369:362–366, 1996.
- [76] R. Adler et al. CPLEAR results on the CP parameters of neutral kaons decaying to $\pi^+ \pi^- \pi^0$. *Phys. Lett. B*, 407:193–200, 1997.
- [77] D. Babusci et al. A new limit on the CP violating decay $K_S \rightarrow 3\pi^0$ with the KLOE experiment. *Phys. Lett. B*, 723:54–60, 2013.

- [78] A. Angelopoulos et al. A Determination of the CPT violation parameter $\text{Re}(\delta)$ from the semileptonic decay of strangeness tagged neutral kaons. *Phys. Lett. B*, 444:52–60, 1998.
- [79] B. Pontecorvo. Inverse beta processes and nonconservation of lepton charge. *Zh. Eksp. Teor. Fiz.*, 34:247, 1957.
- [80] A. Renieri. Possibility of Achieving Very High-Energy Resolution in electron-Positron Storage Rings. <https://lib-extopc.kek.jp/preprints/PDF/1975/7506/7506061.pdf>, 2 1975.
- [81] I. Ya. Protopopov, A. N. Skrinsky, and A. A. Zholents. ENERGY MONOCHROMATIZATION OF PARTICLE INTERACTION IN STORAGE RINGS. 1 1979.
- [82] Alexander A. Zholents. Polarized J/ψ mesons at a tau charm factory with a monochromator scheme. 6 1992.
- [83] V. I. Telnov. Monochromatization of e^+e^- colliders with a large crossing angle. 8 2020.